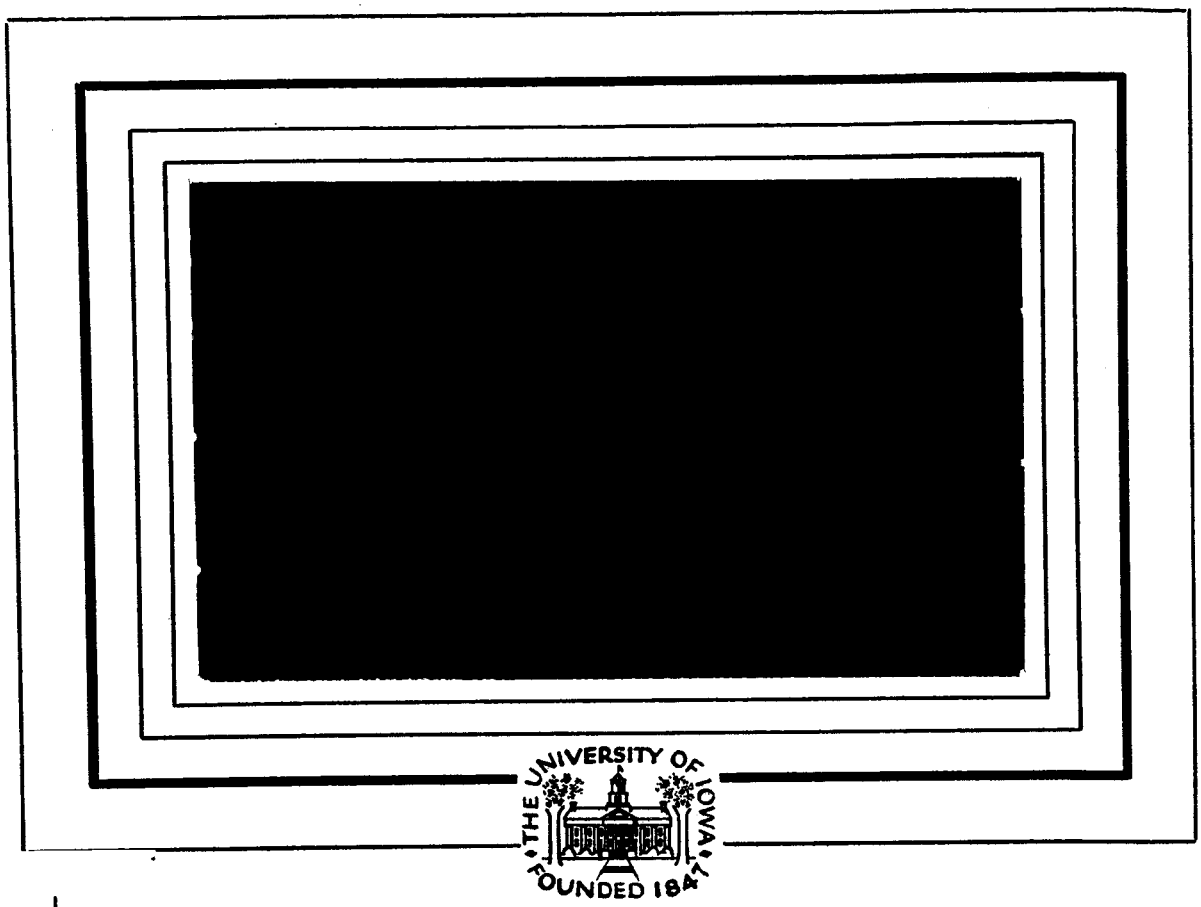

Department of Physics and Astronomy

THE UNIVERSITY OF IOWA

Iowa City, Iowa

U. of Iowa 65-32

Observations of Magnetospheric Boundary Phenomena*

by

L. A. Frank

Department of Physics and Astronomy
University of Iowa
Iowa City, Iowa

August 1965

*To be presented at the Advanced Study Institute "Radiation Trapped in the Earth's Magnetic Field" in Bergen, Norway during August 16--September 3, 1965.

ABSTRACT

12988

A brief summary of recent major observations of magnetospheric boundary phenomena is provided with emphasis on Explorers 12 and 14 and IMP 1 measurements of charged particles and of magnetic fields in the sunward magnetopause region and within the tail of the magnetosphere in the anti-solar direction. Major observations of charged particles in these regions are summarized in several equatorial spatial distribution diagrams.

I. INTRODUCTION

From early observations of auroras [Störmer, 1955] and of cometary tails [Biermann, 1951, 1957] the earth was thought to be immersed in a plasma streaming radially outward from the sun. On the basis of observations of cometary tails and of the solar corona a hydrodynamic model of the solar corona was developed [Parker, 1958] which later proved to be in remarkable agreement with direct measurements [Snyder, Neugebauer, and Rao, 1963] of the solar corpuscular radiation, or solar wind. The advent of the artificial earth satellite and the interplanetary probe provided *in situ* measurements of the environment of the earth in the interplanetary medium: a continual solar plasma directed radially outward from the sun with a bulk velocity of 300-600 km $(sec)^{-1}$ (corresponding proton kinetic energy of $\sim$ 1 keV), a density of $\sim$ 1 to 20 protons $(cm)^{-3}$, and a characteristic temperature of $\sim 10^5$-10^6 °K [Snyder et al., 1963; Bridge et al., 1965], threaded by a weak interplanetary field of $\sim 5\gamma$ ($1\gamma = 10^{-5}$ gauss) forming a general Archimedean spiral structure stretching outward from the sun [Ness and Wilcox, 1965]. The motion of the solar wind past the earth is impeded by the presence of the earth's magnetic field. This interaction of the solar plasma with the geomagnetic field is presumed to be directly related, for example, with the auroras, the geomagnetic storm, and the energetic charged particles of the earth's radiation zones. The solar

wind confines the earth's magnetic field to a cavity, or magnetosphere, which is terminated in the solar direction at ~ 10 R_E (R_E = earth radius) geocentric radial distance [Cahill and Amazeen, 1963; Ness et al., 1964] and is drawn into a magnetic tail extending beyond 30 R_E in the antisolar direction [Ness, 1965] as suggested qualitatively by earlier theoretical models [cf. Piddington, 1959, 1960; Johnson, 1960; Axford and Hines, 1961]. Since the propagation of disturbances (Alfvén waves) in the interplanetary medium can proceed at only a fraction (~ 1/5) of the bulk velocity of the solar plasma, a collisionless magnetohydrodynamic shock should develop on the sunward side of the magnetosphere [cf. Axford, 1962; Kellogg, 1962] and has been directly observed [Ness et al., 1964; Freeman, 1964; Bridge et al., 1965]. Measurements of charged particles near and in the outer magnetosphere have revealed reservoirs of charged particles energized by 'local' acceleration mechanisms driven by the solar wind, for example in the transition region between the shock wave and the sunward magnetospheric boundary and also in the tail of the magnetosphere, which are indicative of charged particle sources for auroral phenomena. The energy flux supplied by the solar wind to the area of the magnetosphere projected toward the sun and available to drive magnetospheric and upper atmospheric phenomena is ~ 10^{20} ergs $(sec)^{-1}$, and is sufficient for supplying the average corpuscular energy flux ~ 10^{18} ergs $(sec)^{-1}$ precipitated into the earth's

upper atmosphere at auroral latitudes [cf. O'Brien, 1964; Frank and Van Allen, 1964a]. In the following presentation the major results of an already substantial and interesting collection of experimental data concerning phenomena in the earth's outer magnetosphere (a complex and variable structure with a volume of at least 10^5 R_E^3) and its immediate vicinity will be discussed.

II. COORDINATE SYSTEMS

A coordinate system for the description of the geomagnetic field direction and magnitude and the spatial and angular distributions of charged particles within the magnetosphere is necessary for the understanding and concise summary of experimental data. Examples of extremely useful coordinates for the summary and analysis of charged particle distributions in the magnetosphere are the familiar B and L coordinates [McIlwain, 1961] based upon the adiabatic invariants of charged particle motion in a magnetic field and measurements of the geomagnetic field at the surface of the earth. This coordinate system provides a two-dimensional map of a three-dimensional spatial distribution of charged particles and temporal changes and longitude nondegeneracies, for example, in the B-L map can be interpreted in terms of the violation of the adiabatic invariants and of sources and sinks of charged particles. Since the flow of solar plasma perturbs the distant geomagnetic field so that an extrapolation of the surface measurements of the geomagnetic field (assuming $\nabla \times \vec{B} = 0$ everywhere external to the earth's surface) becomes inaccurate it is to be expected that this surface-derived B and L coordinate system becomes invalid for the organization of particle intensities in the distant magnetosphere. This situation also becomes more acute as predominant magnetic control of the motion of the charged particle is subdued in the distant magneto-

sphere by electric drifts, by rapid radial diffusion, and by loss and source mechanisms effective in periods less than a longitudinal drift period. Realistic models of the distorted geomagnetic field have been introduced [cf. Hones, 1963; Mead, 1964] and the motions of charged particles in these models [Malville, 1960; Fairfield, 1964] are studied by utilizing the adiabatic invariants in order to separate, for example, the effects of gradient drifts from electric drifts [Hones, 1963; Taylor and Hones, 1965; Taylor, 1965]. Significant perturbation of the observed geomagnetic field from the field as derived from a geomagnetic potential based upon surface measurements begins at 6 to 7 R_E in the magnetic equatorial plane [Cahill and Amazeen, 1963; Ness et al., 1965]. A significant perturbation of the geomagnetic field by the solar wind beyond $L \sim 6$ has also been reflected in the measurements of energetic electrons $E \sim 1.5$ MeV by showing that (a) a nondegeneracy of intensities at a given L as a function of local time [Frank, 1965b] and (b) an asymmetry in observed omnidirectional intensities about the magnetic equator [Frank, 1965a] exist when the surface-derived geomagnetic field is used for the determination of B and L of the positions of the observations. Since the solar wind is responsible for the formation of the magnetosphere (terrestrial ring currents, closed or open, and current sheets will also perturb the distant geomagnetic field) a coordinate system based upon the solar

direction immediately appears appropriate. Such coordinates were first used in the evaluation of Explorer 10 observations of plasma [Bonetti et al., 1963] and magnetic fields [Heppner et al., 1963] and were designated as solar ecliptic coordinates. In the top diagram of Figure 1 is an illustration of this right-handed Cartesian coordinate system (X_{SE}, Y_{SE}, Z_{SE}): $\vec{X}_{SE}$ is parallel to the earth-to-sun direction and $\vec{Z}_{SE}$ is directed toward the North ecliptic pole , θ_{SE} and ϕ_{SE} are the solar ecliptic latitude and longitude, respectively, of point P. For example, in an earth-centered solar ecliptic coordinate system the solar wind vector is directed toward $\theta_{SE} = 0°$, $\phi_{SE} = 180°$ neglecting the aberration effect of $\sim 5°$ due to the earth's revolution about the sun. A more recent coordinate system based upon IMP 1 magnetic measurements in the tail of the magnetosphere has been developed [Ness, 1965] which recognizes the role of the direction of the earth's magnetic moment as well as the solar direction. These coordinates are referred to as solar magnetospheric coordinates (X_{SM}, Y_{SM}, Z_{SM}) (refer to bottom, Figure 1) and are defined with $\vec{X}_{SM}$ parallel to $\vec{X}_{SE}$ and $\vec{Y}_{SM}$ parallel to $\vec{M}_E \times \vec{X}_{SM}$ where $\vec{M}_E$ is parallel to the earth's magnetic dipole axis. In an earth-centered solar magnetospheric coordinate system, for example, a point fixed in celestial coordinates will move in an annual cyclic motion due to the earth's revolution about the sun upon which is superimposed a diurnal motion due to the rotation of the earth. Extensive

surveys of magnetic fields and particle distributions in the tail of the magnetosphere are currently the indicators as to whether magnetic, solar ecliptic, or solar magnetospheric coordinates provide the highest degree of coherency in the organization of the data. A summary of the major experimental observations directed toward this topic is as follows:

(1) The neutral sheet in the earth's magnetic tail is more precisely defined by the solar magnetospheric equatorial plane [Ness, 1965].

(2) Vela satellite measurements of electrons $E > 50$ keV at $\sim 17\ R_E$ show that the occurrence of measurable intensities is preferentially near the magnetic equator rather than near the ecliptic plane or solar magnetospheric equatorial plane [Montgomery et al., 1965].

(3) Explorer 14 measurements of the omnidirectional intensities of electrons $E > 40$ keV near the local midnight meridian indicated a tail of electron intensities lying more nearly in the ecliptic plane than near the geomagnetic equator beyond $10\ R_E$. In fact measurements during a relatively quiescent period in magnetic activity and in intensity temporal variations at similar geomagnetic latitudes but at different ecliptic latitudes repeatedly indicated that geomagnetic latitude was inadequate for

organizing the observed intensities [Frank, 1965a].

(4) The further sophistication of the solar magnetospheric coordinates has not yet proved to be necessary for the organization of shock wave and magnetopause positional data. Solar ecliptic coordinates continue in practice to be adequate for the summary of these data [cf., Ness et al., 1964; Bridge et al., 1965].

It must be remembered in consideration of the above results that the observation of electron intensities $E > 50$ keV in the tail region (for example, (2) above) is not necessarily indicative of the coincident presence of the neutral sheet (1). Further surveys of the electrons and protons in this region of the magnetosphere are necessary in order to pursue the interrelationships of the above results.

III. MEASUREMENTS OF THE DISTANT GEOMAGNETIC FIELD

It is easily recognized that the interpretation of charged particle observations in the earth's magnetosphere and its vicinity depends heavily upon the character of the associated magnetic fields. Major experimental evidences concerning the topology of these magnetic fields are summarized here.

Magnetopause-transition-shock regions. One of the early direct observations of the interaction of the solar wind plasma with the geomagnetic field is shown in Figure 2 as Explorer 12 passed through the magnetospheric boundary, or magnetopause, near the earth-to-sun direction [Freeman, Van Allen, and Cahill, 1963]. The scalar value $|\vec{F}|$ of the observed magnetic field (center, Figure 2) monotonically increases over the Finch and Leaton (1955) extrapolated field with increasing geocentric radial distance while remaining relatively constant in direction. At 52,000 km (8.2 R_E) with $|\vec{F}|$ approximately a factor of 2 larger than the theoretical field a sharp decrease in the magnitude and change of character of the magnetic field occurred and highly disordered magnetic fields with magnitudes of tens of gammas were observed at larger radial distances. Simultaneous observations of charged particles displayed (1) a severe decrease of trapped electron $40 \text{ keV} < E < 50 \text{ keV}$ intensities (SPL-SPB, top, Figure 2) and (2) a large increase of low-energy electrons $\sim$ a few keV of energy

with increasing radial distance concurrent with the above change in the character of the magnetic field. These measurements were interpreted as (1) the termination of durable geomagnetic trapping of charged particles at 8.2 R_E (2) concurrent with the termination of a perturbed but smooth geomagnetic field at the magnetopause with (3) the peak of quasi-thermalized plasma beyond the magnetopause supplying the plasma pressure necessary to balance the magnetic pressure due to the compressed geomagnetic field just inside the magnetopause. These early observations, although not the most detailed available at present, provide a valuable guide to the gross characteristics of the sunward magnetopause region. Although the radial thickness of the persistent quasi-thermalized plasma observed with Explorer 12 was typically 2 to 3 R_E in depth [Freeman, 1964] in agreement with theoretical predictions of the stand-off distance of the bow shock [Kellogg, 1962; Axford, 1962], no observations with the Explorer 12 magnetometer of a change in the character of the magnetic field designating the position of the shock wave were reported. Direct observations of a collisionless magnetohydrodynamic shock wave with a magnetometer were first reported by Ness et al. [1964] with the IMP 1 satellite. An example of these observations is given in Figure 3 which displays the magnetopause at 13.6 R_E and the disordered magnetic field at greater radial distances in the region between the magnetopause and the shock wave. The coordinates θ, ϕ, X_{SE}, Y_{SE}, and Z_{SE}

are satellite-centered solar ecliptic coordinates. At a radial distance of 19.7 R_E and beyond the variances in the magnetic field components of discrete sets of measurements (δX_{SE}, δY_{SE}, δZ_{SE}) become small relative to those within the transition region (or 'magnetosheath') at smaller radial distances and a similar effect is noticeable in the averaged scalar field $\overline{F}$. The change in the character of the magnetic field at 19.7 R_E which is a persistent feature of the IMP 1 measurements beyond the sunward side of the magnetosphere, although variable in position, is interpreted by Ness et al. [1964] as delineating the shock wave boundary. Ness et al. [1964] have summarized their crossings of the magnetopause and shock wave in the ecliptic plane by rotating the observations in a meridian plane containing the Z_{SE} axis and the position of the observation; this summary is reproduced in Figure 4. These data have also been normalized, or rectified, to a geomagnetic latitude of the subsolar point $\chi_{SS} = 0°$. In the ecliptic plane at the subsolar point the average positions of the magnetopause and the shock wave are at ~ 10 R_E and 13.5 R_E and flare out to ~ 13 R_E and 22 R_E, respectively, at $\phi_{SE} = 270°$. The solid lines indicate the result of a theoretical model calculation of the shock position with the magnetospheric boundary used as the blunt body [Spreiter and Jones, 1963]. Calculations of the shape of the sunward magnetopause [cf. Beard, 1960; Midgely and Davis, 1962; Spreiter and Briggs, 1962a, b; Mead and Beard, 1964] are in substantial agreement with these observations.

Explorer 10 observations of the magnetopause toward the tail of the magnetosphere as determined from simultaneous plasma [Bonetti et al., 1963] and magnetic field [Heppner et al., 1963] measurements have been rotated into the ecliptic plane for comparison and strengthen the experimental evidence that no closure of the geomagnetic tail is discernible contrary to closures predicted due to transverse plasma pressures [cf. Johnson, 1960; Beard, 1960].

Motions of the magnetospheric boundary and of the shock wave are implicit in the variations of the measurements summarized in Figure 4 [Ness et al., 1964] and are manifestations of temporal variations in the solar wind densities, velocities, and associated interplanetary magnetic fields. Explorer 10 observations in the evening flank of the magnetosphere over the radial distance range of $\sim 22\ R_E$ to $42\ R_E$ of alternate periods of no plasma and magnetic field directed radially from the sun and of plasma moving generally from the direction of the sun and disordered magnetic fields were interpreted as the motion of the magnetopause across the satellite's position. Freeman [1964] has shown that the correlation of D_{ST} values with the position of the sunward magnetopause as determined by Explorer 12 observations indicates that the magnetosphere is compressed during the initial phase of a magnetic storm presumably by enhanced solar plasma flux and is characterized by a general expansion during the recovery

phase. A single Explorer 12 observation of a transient presence of trapped protons near the magnetopause has given an impulsive, outward radial velocity of the boundary position exceeding 150 km $(sec)^{-1}$ [Konradi and Kaufmann, 1965].

Geomagnetic tail region. The form of the distant geomagnetic field in the anti-solar direction has been of theoretical interest before definitive measurements were available: [cf. Piddington, 1959; Beard, 1960; Axford and Hines, 1961]; active investigations concerning the linear dimensions of the geomagnetic tail in the anti-solar direction are presently continuing [Dessler, 1964; Dungey, 1965; Michel, 1965; Piddington, 1965]. Explorer 10 [Heppner et al., 1963] provided the first direct experimental evidence indicating the nature of the magnetic field topology in the tail of the magnetosphere. Beyond approximately 8 R_E to 22 R_E a magnetic field directed radially outward (the probe was at southerly latitudes during the measurements) from the sun and considerably larger in magnitude over the theoretical values was detected. Beyond 22 R_E the repeated transversal of the magnetopause across the satellite's position occurred. Measurements again at southerly ecliptic latitudes and to a radial distance of $\sim$ 16 R_E with Explorer 14 [Cahill, 1964] provided confirmation of the above Explorer 10 results and indicated a depression of the magnetic field below theoretical values at 7 to 8 R_E. Similar depressions of

the geomagnetic field were observed during the period near solar maximum with Explorer 6 (August 1959) at altitudes as low as 5 R_E /Sonett et al., 1960 a, b; see also Smith, 1963, for a review of Pioneers 1 and 5, Luniks 1 and 2, and Explorers 6 and 10 measurements of the distant magnetic field and the possibility of an associated terrestrial ring current/. The most comprehensive measurements of the magnetic fields in the magnetospheric tail region reported thus far have been obtained by Ness /1965/ with IMP 1 (apogee 31.4 R_E). A representative inbound pass /Ness, 1965/ through the tail region is reproduced in Figure 5; the magnitude $\overline{F}$ and the direction in solar ecliptic coordinates of the measured field are compared with the usual theoretical field (dashed lines). Ness concludes that (1) the large magnetic field of 10 to 30 gammas and characterized by regularity in direction observed to apogee distances (~ half the distance to the lunar orbit) indicate that the earth's magnetic tail extends to at least the lunar orbit and (2) the simultaneous observations of a practically null field and a reversal from anti-solar direction to solar direction of the field at ~ 16 R_E is indicative (supported by similar observations over 18 consecutive orbits) of a neutral sheet in the tail region with a thickness of a fraction of an earth radius. Hence the earth's polar cap lines of force are pulled to the night side of the earth in the

magnetic tail with lines of force from the Northern and Southern Hemispheres directed along the solar and anti-solar directions, respectively, with these two flux tubes separated by a neutral sheet ($B \simeq 0$) containing sufficient plasma to provide a pressure to balance the magnetic pressure of the adjacent tubes of force [see Axford et al., 1964, for a theoretical discussion]. A summary due to Ness [1965] of the magnetic field topology in the noon-midnight meridional plane is shown in Figure 6. Cahill [1965] has recently reported similar results near the midnight meridian which are summarized in Figure 7. The shape of the magnetic field has been projected into a magnetic meridian plane and significant stretching of the field lines in the anti-solar direction appears beyond $\sim 10\ R_E$; observation of a sharp field reversal indicative of the neutral sheet found by Ness was also reported. A coarse comparison [Obayashi, 1965] of the measured magnetic field magnitudes and the extrapolated field along the earth-to-sun line (X_{SE} axis) is given in Figure 8 and illustrates several of the experimental measurements discussed above. The magnetic field topology at high latitudes and large radial distance yet awaits experimental survey.

IV. OBSERVATIONS OF CHARGED PARTICLES IN THE DISTANT GEOMAGNETIC FIELD

The spatial distributions of charged particles surrounding and within the distant geomagnetic field are highly dependent upon the energy and species of charged particles under investigation. An attempt to summarize the major reported evidences provides insight into the complexity of the magnetospheric structure. Other summaries pertaining the the distributions of charged particles within the earth's magnetosphere have been given, for example, by Van Allen [1961], Farley [1963], O'Brien [1963], Frank and Van Allen [1964a], and Obayashi [1965].

Low-energy charged particles. An example of observations of a quasi-thermalized plasma just beyond the magnetopause and compressing the sunward geomagnetic field has been given previously in Figure 2 [Freeman et al., 1963]. The plasma energy flux was of the order of tens of ergs $(cm^2\text{-sec-sr})^{-1}$ and was inferred from rudimentary dynamical considerations to be electrons of energy ~ few kilovolts and intensities $J_{o-} \simeq 10^9 - 10^{10}$ $(cm^2\text{-sec})^{-1}$. Measurements of the proton and electron intensities in this portion of the magnetosphere were continued with a plasma cup on IMP 1 by Bridge and his associates [1964, 1965] and a typical pass is reproduced here in Figure 9. Shown are the average proton energy V, $\log_{10}$ of the total positive ion flux and of the electron flux 65-210 eV looking toward and away from the sun and a measure, T, of the width of the proton distribution. Beyond 15 R_E

the satellite is in the interplanetary medium and a anisotropic flux of protons $J_o \simeq 10^8$ $(cm^2\text{-sec})^{-1}$ is directed away from the sun; the electron intensity 65 eV to 210 eV was reported to be at approximately the noise level of the instrument, $\sim 6 \times 10^6$ $(cm^2\text{-sec})^{-1}$. In the transition region between ~ 10 R_E and 15 R_E approximately isotropic but variable intensities of protons and electrons $J_o \simeq 10^9$ $(cm^2\text{-sec})^{-1}$, a marked increase in ion temperature (measurable intensities in all channels 45 eV through 5400 eV), and a sharp decrease in the intensities of protons and electrons at the magnetopause near 10.5 R_E were observed. These measurements indicate that the proton density in the transition region exceeds the solar wind proton density by a factor of 8 to 10. A summary of the portions of the IMP 1 trajectory along which a hot, approximately isotropic proton flux was observed is shown in Figure 10 [Bridge et al, 1964, 1965]; the transition regions as determined by these plasma observations and by simultaneous magnetic field measurements are coincident (cf. Figure 4 [Ness et al., 1964] of this paper). Wolfe and Silva [1964] generally confirm the above results using a cylindrical analyzer also on IMP 1 and find that the proton angular distributions in the transition region indicate a highly turbulent flow statistically directed away from the sun. Measurements of low-energy electron intensities utilizing a retarding potential analyzer (also IMP 1, one outbound pass) have been obtained by Serbu [1965] and are shown here in Figure 11. The

omnidirectional intensity of electrons $E > 100$ eV is $\sim 2 \times 10^8$ $(cm^2\text{-sec})^{-1}$ from 8 R_E to the position of the shock front at 16 R_E as determined by the magnetometer measurements. Intensities of these electrons decrease sharply at the shock boundary but no change in the observed intensities, increase or decrease, is seen at the magnetopause at $\sim$ 11 R_E. The radial profiles of the omnidirectional intensities of electrons $0 < E < 5$ eV and $5 < E < 10$ eV appear to enjoy a similar independence of the magnetospheric boundary.

A summary of the observations of the low-energy charged particle distributions near the sunward magnetopause as discussed above and in the tail of the magnetosphere is given in Figure 12. The ecliptic plane has been selected here for mapping and comparing the results. Explorer 10 plasma observations [Bonetti et al., 1964] indicate that the plasma resumes supersonic flow along the flanks of the magnetosphere. Observations of low-energy electron $E \gtrsim 100$ eV intensities by Lunik 2 [Gringauz et al., 1961], Explorer 12 [Freeman, 1963], and Mars 1 [Gringauz et al., 1964] beyond ~ 8 R_E are in coarse agreement although there is an obvious need for more definitive measurements. The results of Gringauz and his collaborators [1964] at high latitudes ($\lambda_m \sim 50°$) (for coordinates, see Vakulov et al., [1964]) have been coarsely translated into the ecliptic plane by direct L-shell mapping. The position of these large electron intensities agrees with the onset of change in character of the geomagnetic field

in the anti-solar direction measured with IMP 1 and Explorer 14 as reviewed above. The observed electron energy flux of several tens of ergs $(cm^2\text{-sec})^{-1}$ (energy density $\sim 10^{-8}$ ergs $(cm)^{-3}$ if E $\sim$ a few kilovolts) appears sufficient to support the neutral sheet discovered by Ness [1965] if B $\sim$ 30 gammas for the magnitude of the adjacent fields. Large intensities of electrons of similar energies at low altitudes and high latitudes L $\gtrsim$ 8 have been observed during local night [Sharp et al., 1965; Fritz and Gurnett, 1965] and further suggest the tail region as at least a partial reservoir and/or accelerating region for auroral particles. The spatial connection of the two regions characterized by large intensities of electrons E > 100 eV near the sunward magnetopause and in the geomagnetic tail has not been determined [cf. Gringauz, 1964; Van Allen, 1964] and further surveys in the dawn, evening, and tail portions of the magnetosphere are necessary to establish the relationship.

Medium-energy charged particles. Simultaneous measurements of magnetic fields and electron E $\sim$ 50 keV intensities with Explorer 12 revealed that a large decrease of electron intensities occurred concurrently with the disappearance at the sunward magnetopause of the uniform, although perturbed, geomagnetic field necessary for the durable trapping of charged particles [Freeman et al., 1963]

(refer to present Figure 2). Another example of the typical behavior of the radial profiles of electron E > 40 keV, E > 230 keV, and E > 1.6 MeV intensities near the sunward magnetospheric boundary with Explorer 14 [Frank and Van Allen, 1964b] is given in the left-hand inset of Figure 13. The "spikes" of electron E > 40 keV intensities beyond the position of the trapping boundary at ~ 70,000 km and extending in this example to ~ 93,000 km in the general vicinity of the transition region have been observed by Anderson et al. [1965], Frank and Van Allen [1964b], and Fan et al. [1964] and are suggestive of a high-energy tail of the electron spectrums in the transition region (J_o (E > 40 keV)/J_o (E $\gtrsim$ 1 keV) ~ 10^{-5}) [Frank and Van Allen, 1964b]. Theoretical hypotheses for the acceleration of these energetic electrons have been given by Scarf et al. [1965] and Jokipii and Davis [1964]. A coarse positive correlation of the occurrence of these intensity 'spikes' with the planetary magnetic index K_p (right-hand inset Figure 13) was found [Frank and Van Allen, 1964b] with average K_p values $\simeq$ 2.5 and $\simeq$ 1.5 for passes with and without intensity spikes beyond the magnetopause, respectively. The percentage of passes with observations of spikes while the satellite was in the transition region and K_p was 3 or 4 (~ 20 passes) was ~ 75%. Figure 13 also displays the 'flaring' of the magnetospheric boundary as deduced

from the characteristic sharp termination of intensities in general agreement with IMP 1 magnetic field measurements [Ness et al., 1964] and the increasing thickness of the regions with extra-magnetospheric spikes with angular displacement from the subsolar point [Frank et al., 1963; Fan et al., 1964; Frank and Van Allen, 1964b; Anderson et al., 1965]. Direct correlation of the position of the shock as determined by simultaneous magnetic field measurements with the positions of these intensity spikes shows that the intensity spikes are not coincident with, but are also sometimes positioned upstream from, the position of the shock wave [Anderson et al., 1965; Jokipii and Davis, 1964]. The interpretation due to Anderson et al. [1965] of small intensity spikes ($\sim 10^3$ to 10^4 $(cm^2\text{-sec})^{-1}$) observed at large distances in front of the shock as being of terrestrial origin may be complicated by the recent discovery [Van Allen and Krimigis, 1965] of solar electron E $\sim$ 40 keV events with Mariner 4 data.

A summary of several gross features of the spatial distributions of electrons E $\sim$ 40 keV is given in Figure 14. A rough upper limit of the average electron E > 40 keV intensity in the interplanetary medium is ~ 10 $(cm^2\text{-sec})^{-1}$ as determined with Mariner 4 [cf. Van Allen, 1965]. Surrounding the earth and extending to the magnetopause in the solar direction (~ 10 R_E) and to ~ 8 R_E in the anti-solar direction is a 'hard core' of electron E > 40 keV intensities

$\sim 10^7$-10^8 $(cm^2\text{-sec})^{-1}$ characterized by relatively weak temporal and spatial variations when compared to outlying regions of the magnetosphere [Frank, 1965a]. Within 45° of longitude of the subsolar point at low latitudes these intensities are terminated coincidently with the magnetopause. In the dawn and evening 'skirts' of the spatial (i.e., at larger angular displacements from the subsolar point) distribution tortuous temporal and spatial variations are observed [Frank et al., 1963; Anderson et al., 1965; Frank, 1965a] and their association with the magnetopause in terms of spatially correlated decreases or increases in intensity weakens and disappears toward the flanks of the magnetosphere [Anderson et al., 1965]. Montgomery et al. [1965] have noted a large asymmetry in the dawn and evening skirts with the dawn skirt having generally more intense and frequent electron E > 50 keV intensity spikes when compared with observations in the local evening skirt. Observations with Explorer 14 displayed no significant dawn-evening asymmetry during relatively quiescent magnetic conditions ($\sum K_p \leq 25$) [Frank, 1965a] but the nearly circular Vela orbits [Montgomery et al., 1965] are more favorable for observing such an asymmetry than the highly eccentric Explorer 14 orbit. In the anti-solar direction a 'tail' of electron E > 40 keV intensities has been found [Frank, 1965a; Anderson, 1965] characterized by much weaker temporal and spatial

dependences when compared to those of the skirt regions and a shallow latitude dependence compared to that of the 'core' of intensities. The position of this 'tail' of electron intensities presumably is coincident with the neutral sheet. Anderson [1965] has found 'spikes' of intensities with fast risetimes (~ a few minutes) with approximately exponential decays (~ a few minutes to hours) in the anti-solar direction to at least IMP 1 apogee position of ~ 32 R_E with a strong decrease in frequency of occurrence with increasing radial distance and infers that these 'islands' (typically several R_E in linear dimensions) are impulsively injected into the tail region. Asbridge et al. [1965] have observed electrons of similar energies streaming in the anti-solar direction in the geomagnetic tail at ~ 17 R_E. Recently intensity 'spikes' of low-energy protons E > 125 keV, $j \simeq 10^3$ to 10^4 $(cm^2\text{-sec-sr})^{-1}$ in these regions have been reported [Konradi, 1965]. Observations of rapid increases of intensities during the onsets of several intensity 'spikes' in the evening skirt of intensities with OGO 1 allowed Frank et al. [1965] to set a lower limit on the bulk velocity of the irregularities of 50 km $(sec)^{-1}$. A coarse summary of the average omnidirectional intensities of electrons E > 40 keV as a function of geocentric radial distance in the anti-solar direction is shown in Figure 15 which includes the Explorer 14 and IMP 1 data

discussed above and a single determination at 3300 R_E with Mariner 4 [Van Allen, 1965]; average intensities at the lunar orbit in the anti-solar direction might reasonably be expected to be $\sim 10^3$ $(cm^2\text{-sec})^{-1}$.

Periodic variations of the intensities of electrons E > 40 keV with periods ~ 6 minutes and persisting for several hours in the skirt and tail regions of the magnetosphere have been recently reported [Anderson, 1965]. These variations are presumably related to periodic variations in the magnetic field (cyclic acceleration and deceleration by hydromagnetic waves) such as the long-period hydromagnetic waves observed by Patel [1965] (for theoretical discussions of the generation and propagation of magnetospheric hydromagnetic waves, refer to Dessler [1958, 1961], Dessler and Parker [1959], Dessler and Walters [1964], and MacDonald [1961]).

Energetic electrons. The spatial distributions of electron $E \gtrsim 1.5$ MeV intensities in the outer magnetosphere and beyond are summarized in Figure 16. The isopleths of constant intensities $J_o = 10^2, 10^3, 10^4$ $(cm^2\text{-sec})^{-1}$ as measured with Explorer 14 near the magnetic equatorial plane exhibit a large local time dependence in radial position (for example, the isopleth $J_o = 10^2$ $(cm^2\text{-sec})^{-1}$ is positioned at 10 R_E in the solar direction and at 8 R_E in the anti-solar direction) and the spatial distribution of these energetic electrons lies within the relatively

stable 'core' of 40 keV electron intensities (see Figure 14) [Frank, 1965b]; this region as defined by the outermost contour is probably indicative of the region in which complete longitudinal drift paths around the earth are possible. Several intensity spikes of electrons E > 1.5 MeV ($J_o \sim 10$ $(cm^2\text{-sec})^{-1}$) were observed in the dawn skirt and transition region and none in the corresponding evening portions of the magnetosphere but the statistics are poor with only several events of observable intensity discovered in the data. Arrows on the isopleths indicate excursions (temporal variations) in the position of the contour $J_o = 10^2$ $(cm^2\text{-sec})^{-1}$ observed with Explorer 14. Upper limits on the average interplanetary omnidirectional intensities are $\overline{J_o}$ (> 3 MeV) $\lesssim 0.1$ $(cm^2\text{-sec})^{-1}$ [Cline et al., 1964] and $\overline{J_o}$ (> 1.5 MeV) $\lesssim 1$ $(cm^2\text{-sec})^{-1}$ [Frank, private communication] with IMP 1 and Explorer 14 data, respectively.

The diurnal variation of electron E > 280 keV intensities observed at low altitudes $L \gtrsim 6$ [Williams and Palmer, 1965] is in qualitative agreement with the observations of electrons E > 1.5 MeV in the magnetic equatorial plane [Frank, 1965b] and is consistent with the motion of charged particles in models of the perturbed geomagnetic field [cf. Hones, 1963].

Determinations of the isopleths of electron E > 1.5 MeV intensities [Frank, 1965b] in the outer magnetosphere indicate

that the axis of symmetry of the local time distribution of charged particles may not be the earth-to-sun direction but may lie closer to the 11:00-23:00 (local time) meridional plane. Although this single result is inconclusive, a similar effect has been observed in the diurnal variations of electron $E > 40$ keV intensities at low altitudes with Injun 3 data [Frank et al., 1967].

ACKNOWLEDGEMENTS

The research was supported in part by the National Aeronautics and Space Administration under Grant NsG-233-62 and by the Office of Naval Research under Contract Nonr 1509(06).

REFERENCES

Anderson, K. A., Energetic electron fluxes in the tail of the geomagnetic field, J. Geophys. Res. (to be published 1965).

Anderson, K. A., H. K. Harris, and R. J. Paoli, Energetic electron fluxes in and beyond the earth's outer magnetosphere, J. Geophys. Res., 70, 1039, 1965.

Asbridge, J. R., S. J. Bame, H. E. Felthauser, R. H. Olson, and I. B. Strong, Streaming of electrons and protons in the earth's magnetospheric tail at 17 earth radii, Trans. Am. Geophys. Union, 46 (1), 142, 1965.

Axford, W. I., The interaction between the solar wind and the earth's magnetosphere, J. Geophys. Res., 67, 3791, 1962.

Axford, W. I., and C. O. Hines, A unifying theory of high-latitude geophysical phenomena and geomagnetic storms, Can. J. Phys., 39, 1322, 1961.

Axford, W. I., H. E. Petschek, and G. L. Siscoe, Tail of the magnetosphere, J. Geophys. Res., 70, 1231-1236, 1965.

Beard, D. B., The interaction of the terrestrial magnetic field with the solar corpuscular radiation, J. Geophys. Res., 65, 3559, 1960.

Biermann, L., Kometenschweife und solar korpuskularstrahlung, Z. Astrophys., 29, 274, 1951.

Biermann, L., Solar corpuscular radiation and the interplanetary gas, Observatory, 77 (898), 109, 1957.

Bonetti, A., H. S. Bridge, A. J. Lazarus, B. Rossi, and F. Scherg, Explorer 10 plasma measurements, J. Geophys. Res., 68, 4017, 1963.

Bridge, H., A. Egidi, A. Lazarus, E. Lyon, and L. Jacobson, Preliminary results of plasma measurements on IMP-A, Space Research V, North-Holland Publishing Company, 969, 1965.

Bridge, H. S., A. Egidi, A. Lazarus, E. F. Lyon, L. Jacobson, and R. H. Baker, Initial results from the first Interplanetary Monitoring Platform (IMP-I), Trans. Am. Geophys. Union, 45 (3), 515, 1964.

Cahill, L. J., Preliminary results of magnetic field measurements in the tail of the geomagnetic cavity, Trans. Am. Geophys. Union, 45 (1), 231, 1964.

Cahill, L. J., Inflation of the magnetosphere near 8 earth radii in the dark hemisphere, U. of New Hampshire Research Report 65-4, 1965.

Cahill, L. J., and P. G. Amazeen, The boundary of the geomagnetic field, J. Geophys. Res., 68, 1835, 1963.

Cline, T. L., G. H. Ludwig, and F. B. McDonald, Detection of interplanetary 3- to 12-MeV electrons, Phys. Rev. Letters, 13 (26), 786, 1964.

Dessler, A. J., Large amplitude hydromagnetic waves above the ionosphere, J. Geophys. Res., 63, 507, 1958.

Dessler, A. J., The stability of the interface between the solar wind and the geomagnetic field, J. Geophys. Res., 66, 3587, 1961.

Dessler, A. J., Length of magnetospheric tail, J. Geophys. Res., 69, 3913, 1964.

Dessler, A. J., and E. N. Parker, Hydromagnetic theory of geomagnetic storms, J. Geophys. Res., 64, 2239, 1959.

Dessler, A. J., and G. K. Walters, Hydromagnetic coupling between solar winc and magnetosphere, Planetary and Space Science, 12, 227, 1964.

Dungey, J. W., The length of the magnetospheric tail, J. Geophys. Res., 70, 1753, 1965.

Fan, C. Y., G. Gloeckler, and J. A. Simpson, Evidence for > 30 keV electrons accelerated in the shock transition region beyond the earth's magnetospheric boundary, Phys. Rev. Letters, 13, 149, 1964.

Farley, T. A., The growth of our knowledge of the earth's outer radiation belt, Rev. Geophys., 1, 3, 1963.

Fairfield, D. H., Trapped particles in a distorted dipole field, J. Geophys. Res., 69, 3919, 1964.

Frank, L. A., A survey of electrons E > 40 keV beyond 5 earth radii with Explorer 14, J. Geophys. Res., 70, 1593, 1965a.

Frank, L. A., On the local-time dependence of outer radiation zone electron (E > 1.6 MeV) intensities near the magnetic equator, J. Geophys. Res., 70, 4131-4138, 1965b.

Frank, L. A., and J. A. Van Allen, A survey of magnetospheric boundary phenomena, Chapter 7, pp. 161-187 of Research in Geophysics. Volume 1: Sun, Upper Atmosphere and Space, edited by H. Odishaw, M.I.T. Press, 1964a.

Frank, L. A., and J. A. Van Allen, Measurements of energetic electrons in the vicinity of the sunward magnetospheric boundary with Explorer 14, J. Geophys. Res., 69, 4923, 1964b.

Frank, L. A., J. A. Van Allen, and J. D. Craven, Large diurnal variations of geomagnetically trapped and of precipitated electrons observed at low altitudes, J. Geophys. Res., 69, 3155-3167, 1964.

Frank, L. A., J. A. Van Allen, and E. Macagno, Charged particle observations in the earth's outer magnetosphere, J. Geophys. Res., 68, 3543, 1963.

Frank, L. A., J. A. Van Allen, H. K. Hills, and R. W. Fillius, Proton and electron intensities in the earth's outer radiation zone: OGO 1 (title), Trans. Am. Geophys. Union, 46 (1), 124, 1965.

Freeman, John W., Jr., The morphology of the electron distribution in the outer radiation zone and near the magnetospheric boundary as observed by Explorer 12, J. Geophys. Res., 69, 1691, 1964.

Freeman, J. W., J. A. Van Allen, and L. J. Cahill, Jr., Explorer 12 observations of the magnetospheric boundary and the associated solar plasma on September 13, 1961, J. Geophys. Res., 68, 2121, 1963.

Fritz, T. A., and D. A. Gurnett, Diurnal and latitudinal effects observed for 10 keV electrons at low satellite altitudes, J. Geophys. Res., 70, 2485, 1965.

Gringauz, K. I., Remarks on papers by J. W. Freeman, J. A. Van Allen, and L. J. Cahill, "Explorer 12 observations of the magnetospheric boundary and the associated solar plasma on September 13, 1961" and by L. A. Frank, J. A. Van Allen, and E. Macagno, "Charged particle observations in the earth's outer magnetosphere", J. Geophys. Res., 69, 1007, 1964.

Gringauz, K. I., V. V. Bezrukikh, L. S. Musatov, R. E. Rybchinsky, and S. M. Sheronova, Measurements made in the earth's magnetosphere by means of charged particle traps aboard the Mars 1 probe, Space Research IV, North-Holland Publishing Company, Amsterdam, 621, 1964.

Gringauz, K. I., V. G. Kurt, V. I. Moroz, and I. S. Shklovskii, Results of observations of charged particles observed out to R = 100,000 km, with the aid of charged-particle traps on Soviet space rockets, Astron. Zh., 37, 716 (1960; translation in: Soviet Astronomy-A.J, 4, 680 1961).

Heppner, J. P., N. F. Ness, C. S. Scearce, and T. L. Skillman, Explorer 10, magnetic field measurements, J. Geophys. Res., 68, 1-46, 1963.

Hones, E. W., Motions of charged particles trapped in the earth's magnetosphere, J. Geophys. Res., 68, 1209, 1963.

Jokipii, J. R., and L. Davis, Jr., Acceleration of electrons near the earth's bow shock, Phys. Rev. Letters, 13, 739, 1964.

Johnson, F. S., The gross character of the geomagnetic field in the solar wind, J. Geophys. Res., 65, 3049, 1960.

Kellogg, P. J., Flow of plasma around the earth, J. Geophys. Res., 67, 3805, 1962.

Konradi, A., Electron and proton distributions in the anti-solar direction as seen by Explorer 14 and OGO 1 (title), Trans. Am. Geophys. Union, 46, (1), 124, 1965.

Konradi, A., and R. L. Kaufmann, Evidence for rapid motion of the outer boundary of the magnetosphere, J. Geophys. Res., 70, 1627, 1965.

MacDonald, G. J. F., Spectrum of hydromagnetic waves in the exosphere, J. Geophys. Res., 66, 3639, 1961.

McIlwain, C. E., Coordinates for mapping the distribution of magnetically trapped particles, J. Geophys. Res., 66, 3681-3692, 1961.

Malville, J. M., The effect of the initial phase of a magnetic storm upon the outer Van Allen belt, J. Geophys. Res., 65, 3008, 1960.

Mead, G. D., Deformation of the geomagnetic field by the solar wind, J. Geophys. Res., 69, 1181, 1964.

Mead, G. D., and D. B. Beard, Shape of the geomagnetic field solar wind boundary, J. Geophys. Res., 69, 1169, 1964.

Michel, F. C., Detectability of disturbances in the solar wind, J. Geophys. Res., 70, 1, 1965.

Midgley, J. E., and L. Davis, Computation of the bounding surface of a dipole field in a plasma by a moment technique, J. Geophys. Res., 67, 499, 1962.

Montgomery, M. D., S. Singer, J. P. Conner, and E. E. Stogsdill, Spatial distribution, energy spectra, and time variations of energetic electrons (E > 50 keV) at 17.7 earth radii, Phys. Rev. Letters, 14 (7), 209, 1965.

Ness, N. F., The earth's magnetic tail, J. Geophys. Res., 70, 2989, 1965.

Ness, N. F., C. S. Scearce, and J. B. Seek, Initial results of the IMP-1 magnetic field experiment, J. Geophys. Res., 69, 3531, 1964.

Ness, N. F., and J. M. Wilcox, Solar origin of the interplanetary magnetic field, Phys. Rev. Letters, 13 (15), 461-464.

Obayashi, T., The magnetosphere and its boundary, NASA Tech. Note NASA TN D-2789, 1965.

O'Brien, B. J., Review of studies of trapped radiation with satellite-borne apparatus, Space Sci. Rev., 1, 415, 1962-1963.

O'Brien, B. J., High-latitude geophysical studies with satellite Injun 3. 3. Precipitation of electrons into the atmosphere, J. Geophys. Res., 69, 13, 1964.

Patel, V. L., Long period hydromagnetic waves in the magnetosphere: Explorer 14, U. of New Hampshire Res. Report 65-3, 1965.

Parker, E. N., Dynamics of the interplanetary gas and magnetic fields, Astrophys. J., 128, 664, 1958.

Piddington, J. H., The transmission of geomagnetic disturbances through the atmosphere and interplanetary space, Geophys. J., 2, 173, 1959.

Piddington, J. H. Geomagnetic storm theory, J. Geophys. Res., 65, 93, 1960.

Piddington, J. H., The geomagnetic tail and magnetic storm theory, Planet, Space Sci., 13, 281, 1965.

Scarf, F. L., W. Bernstein, and R. W. Fredricks, Electron acceleration and plasma instabilities in the transition region, J. Geophys. Res., 70, 9, 1965.

Serbu, G. P., Results from the IMP-1 retarding potential analyzer, Space Research V, North-Holland Publishing Company, Amsterdam, 564, 1965.

Sharp, R. D., J. E. Evans, W. L. Imhof, R. G. Johnson, J. B. Reagan, and R. V. Smith, Satellite measurements of low-energy electrons in the northern auroral zone, J. Geophys. Res., 69, 2721, 1964.

Smith, E. J., Theoretical and experimental aspects of ring currents, Space Science, D. P. LeGalley (ed.), 316 (Wiley and Sons, 1963).

Snyder, C. W., M. Neugebauer, and U. R. Rao, The solar wind velocity and its correlation with cosmic ray variations and with solar and geomagnetic activity, J. Geophys. Res., 68, 6361, 1963.

Sonett, C. P., E. J. Smith, D. L. Judge, and P. J. Coleman, Phys. Rev. Letters, 4, 161, 1960.

Sonett, C. P., E. J. Smith, and A. R. Sims, Space Research I, ed. H. K. Kallmann-Bijl, North-Holland Publishing Company, Amsterdam, 962, 1960.

Spreiter, J. R., and B. R. Briggs, On the choice of condition to apply at the boundary of the geomagnetic field in the steady-state Chapman-Ferraro problem, J. Geophys. Res., 67, 2983, 1962a.

Spreiter, J. R., and B. R. Briggs, Theoretical determination of the form of the hollow produced in the solar corpuscular stream by interaction with the magnetic dipole field of the earth, J. Geophys. Res., 67, 2985, 1962b.

Spreiter, J. R., and W. P. Jones, On the effect of a weak interplanetary magnetic field on the interaction between the solar wind and the geomagnetic field, J. Geophys. Res., 68, 3555, 1963.

Störmer, C., The Polar Aurora, The Clarendon Press, 1955.

Taylor, H. E., Calculations of charged particle motions for a model atmosphere using the adiabatic invariants, Fifth Western Am. Geophys. Union Meeting (abstract), Dallas, Texas, 1965.

Taylor, H. E., and E. W. Hones, Adiabatic motion of auroral particles in a model of the electric and magnetic field surrounding the earth, J. Geophys. Res., 70, 3605, 1965.

Vakulov, P. V., S. N. Vernov, E. B. Gorchakov, Yu. I. Logachev, A. N. Charakhchyan, T. N. Charackhchyan, and A. E. Chudakov, Investigation of cosmic rays, Space Research IV, North-Holland Publishing Company, Amsterdam, 26, 1964.

Van Allen, J. A., Dynamics, composition and origin of the geomagnetically-trapped corpuscular radiation, Trans. Intern. Astronom. Union, 11B, 99, 1962.

Van Allen, J. A., Remarks on accompanying letter by K. I. Gringauz, J. Geophys. Res., 69, 1011, 1964.

Van Allen, J. A., Absence of 40 keV electrons in the earth's magnetospheric tail at 3300 earth radii, J. Geophys. Res., 70, October 1, 1965.

Van Allen, J. A., and S. M. Krimigis, Impulsive emission of ~ 40 keV electrons from the sun, (submitted for publication, J. Geophys. Res., 1965).

Williams, D. J., and W. F. Palmer, Distortions in the radiation cavity as measured by an 1100-kilometer polar orbiting satellite, J. Geophys. Res., 70, 557, 1965.

Wolfe, J. H., and R. W. Silva, Initial results from the first Interplanetary Monitoring Platform (IMP-I), Trans. Am. Geophys. Union, 45 (3), 512, 1964.

FIGURE CAPTIONS

Figure 1. Illustrations of the solar ecliptic coordinate system (upper diagram) and of the solar magnetospheric coordinate system (lower diagram).

Figure 2. Particle and magnetic field measurements with Explorer XII for the inbound pass on 13 September 1961. The CdSB (magnet in aperture) detector count-rate has been normalized to the energy scale of the CdSTE (no magnet in aperture) detector. The counting rates of both CdS detectors are nearly linear with energy flux. Both spectrometer channels (SpL and SpH) have been corrected for background counts by the subtraction of the counting rate of the background detector SpB. The CdS optical monitor (not shown) indicated that during this pass the CdS detectors did not have any bright objects within their field of view. F denotes the scalar magnetic field strength; α the angle between the F-vector and the spin-axis of the satellite; and ψ the dihedral angle between the plane containing the F-vector and the spin axis and the plane containing the spin axis and the satellite-sun line (after Freeman et al. [1963]).

Figure 3. Magnetic field data (IMP 1) from orbit No. 11 January 5, 1964, illustrating outbound traversal of magnetopause boundary at 13.6 R_E and shock wave boundary at 19.7 R_E (after Ness et al. [1964]).

Figure 4. Summary of location of rectified shock wave and magnetopause boundary crossings and comparison with theoretical predictions using analogy with supersonic fluid flow (after Ness et al. [1964]).

Figure 5. Magnetic field data from inbound orbit No. 41, May 2 through May 4, 1964. Throughout most of this time interval the magnetic field is pointed anti-solar although at a geocentric distance of 16 R_E the magnetic field abruptly reverses direction at the same time that it becomes very weak or zero. This spatially limited region is identified as a neutral sheet in the earth's magnetic tail (after Ness [1965]).

Figure 6. Illustration of the interpretation of the IMP 1 magnetic field data field topology within the noon-midnight meridian plane. The relative position of the neutral surface or sheet in the earth's magnetic tail and the corotating magnetic field lines supporting trapped particle motion are indicated. These include the classical Van Allen radiation belts. The collisionless shock and magnetosphere boundaries are extrapolated to the polar regions indicating a depression but the relative position of a polar neutral point and the size of the boundary are not experimentally determined. Cylindrical symmetry about the earth-sun line has been assumed for the boundary of the earth's magnetic tail in this presentation (after Ness [1965]).

Figure 7. A schematic representation of the magnetic lines of force projected upon a magnetic meridional plane as observed by Explorer 14 near local midnight (after Cahill [1965]).

Figure 8. Schematic representation of the outer geomagnetic field in the equatorial plane along the sun-earth line (after Obayashi [1965]).

Figure 9. Measurements of low-energy protons and electrons in the transition region and in the interplanetary medium with a Faraday cup type instrument on IMP 1 (after Bridge et al. [1965]).

Figure 10. Summary of portions of IMP 1 trajectory during which a hot, nearly isotropic plasma flux was observed (after Bridge et al. [1965]).

Figure 11. Plot of low-energy electron fluxes as a function of geocentric radial distance (after Serbu [1965]).

Figure 12. Coarse summary of low-energy charged particle observations. Average positions of the magnetopause and the shock as given by Ness [1965] have been included in the diagram.

Figure 13. Summary of Explorer 14 observations of the sharp termination of electron $E > 40$ keV intensities at the sunward magnetopause and of the intensity 'spikes' in and near the transition region (after Frank and Van Allen [1964b]).

Figure 14. Coarse summary of the observations of electrons $E > 40$ keV near the ecliptic plane.

Figure 15. Summary of the observations of electron $E > 40$ keV intensities as a function of radial distance in the anti-solar direction.

Figure 16. Coarse summary of the observations of electron $E > 1.6$ MeV intensities in the magnetic equatorial plane.

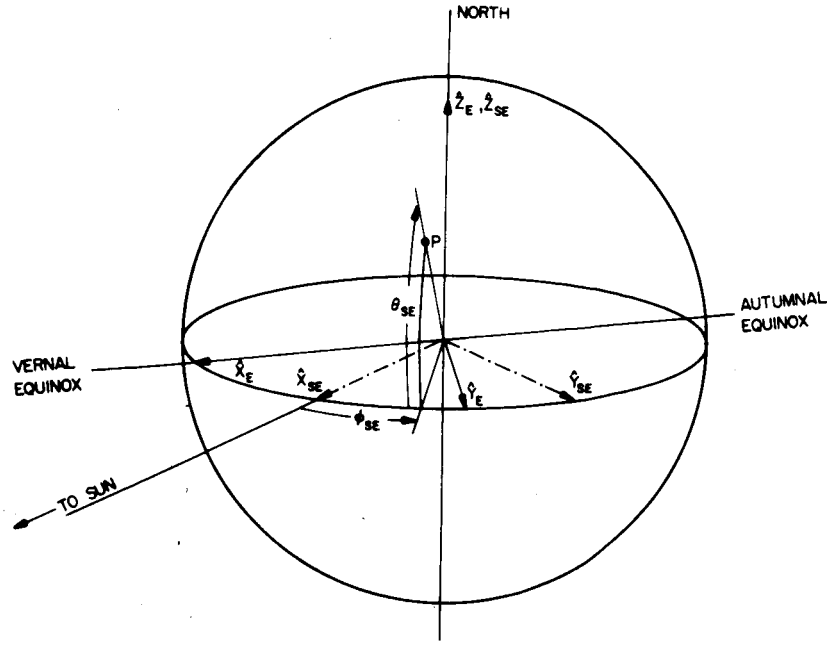

$\hat{X}_E, \hat{Y}_E, \hat{Z}_E$ ECLIPTIC

$\hat{X}_{SE}, \hat{Y}_{SE}, \hat{Z}_{SE}$ SOLAR ECLIPTIC

θ_{SE} SOLAR ECLIPTIC LATITUDE

ϕ_{SE} SOLAR ECLIPTIC LONGITUDE

SOLAR ECLIPTIC COORDINATE SYSTEM

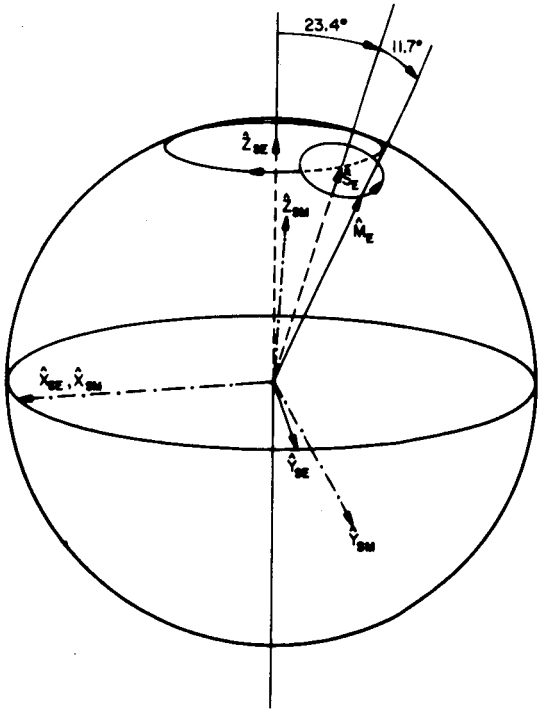

$\hat{M}_E$ ∥ EARTH'S MAGNETIC DIPOLE AXIS

$\hat{S}_E$ ∥ EARTH'S SPIN AXIS

$\hat{X}_{SM}, \hat{Y}_{SM}, \hat{Z}_{SM}$ SOLAR MAGNETOSPHERIC

$\hat{X}_{SM} \parallel \hat{X}_{SE}$

$\hat{Y}_{SM} \parallel \hat{M}_E \times \hat{X}_{SM}$

SOLAR MAGNETOSPHERIC COORDINATE SYSTEM

Figure 1

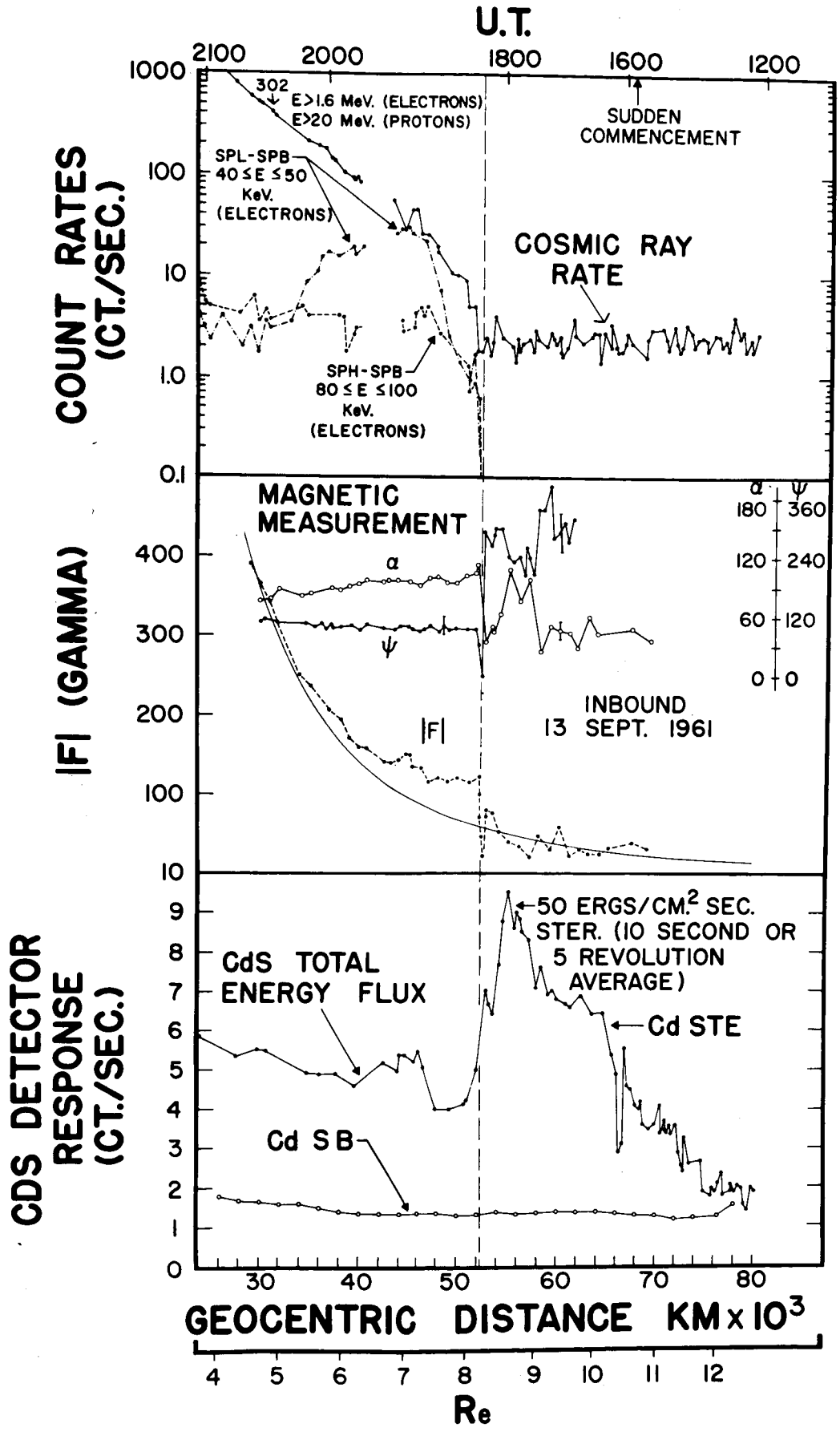
U.T.
2100
2000
1800
1600
1200
1000
100
10
1.0
0.1
COUNT RATES (CT./SEC.)
302
E>1.6 MeV. (ELECTRONS)
E>20 MeV. (PROTONS)
SUDDEN COMMENCEMENT
SPL-SPB
40 ≤ E ≤ 50
KeV.
(ELECTRONS)
COSMIC RAY RATE
SPH-SPB
80 ≤ E ≤ 100
KeV.
(ELECTRONS)
400
300
200
100
10
|F| (GAMMA)
MAGNETIC MEASUREMENT
α
ψ
|F|
180
120
60
0
360
240
120
0
INBOUND
13 SEPT. 1961
9
8
7
6
5
4
3
2
1
0
CDS DETECTOR RESPONSE (CT./SEC.)
CdS TOTAL ENERGY FLUX
50 ERGS/CM.2 SEC. STER. (10 SECOND OR 5 REVOLUTION AVERAGE)
Cd STE
Cd S B
30
40
50
60
70
80
GEOCENTRIC DISTANCE KM x 10^3
4
5
6
7
8
9
10
11
12
Re

Figure 2

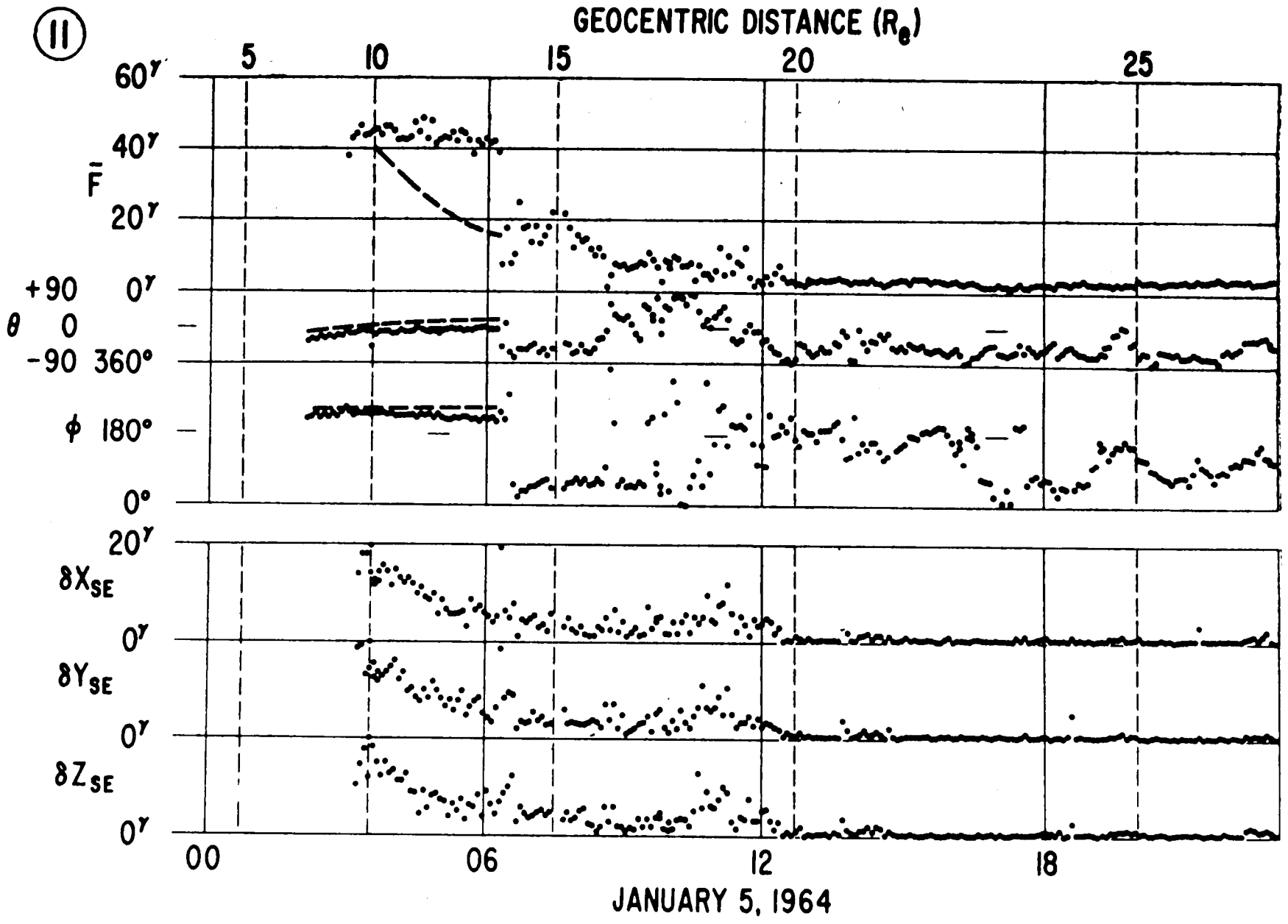
(11)
GEOCENTRIC DISTANCE (R_e)
5
10
15
20
25
60γ
40γ
$\bar{F}$
20γ
0γ
+90
θ 0
-90
360°
φ 180°
0°
20γ
δX_{SE}
0γ
δY_{SE}
0γ
δZ_{SE}
0γ
00
06
12
18
JANUARY 5, 1964

Figure 3

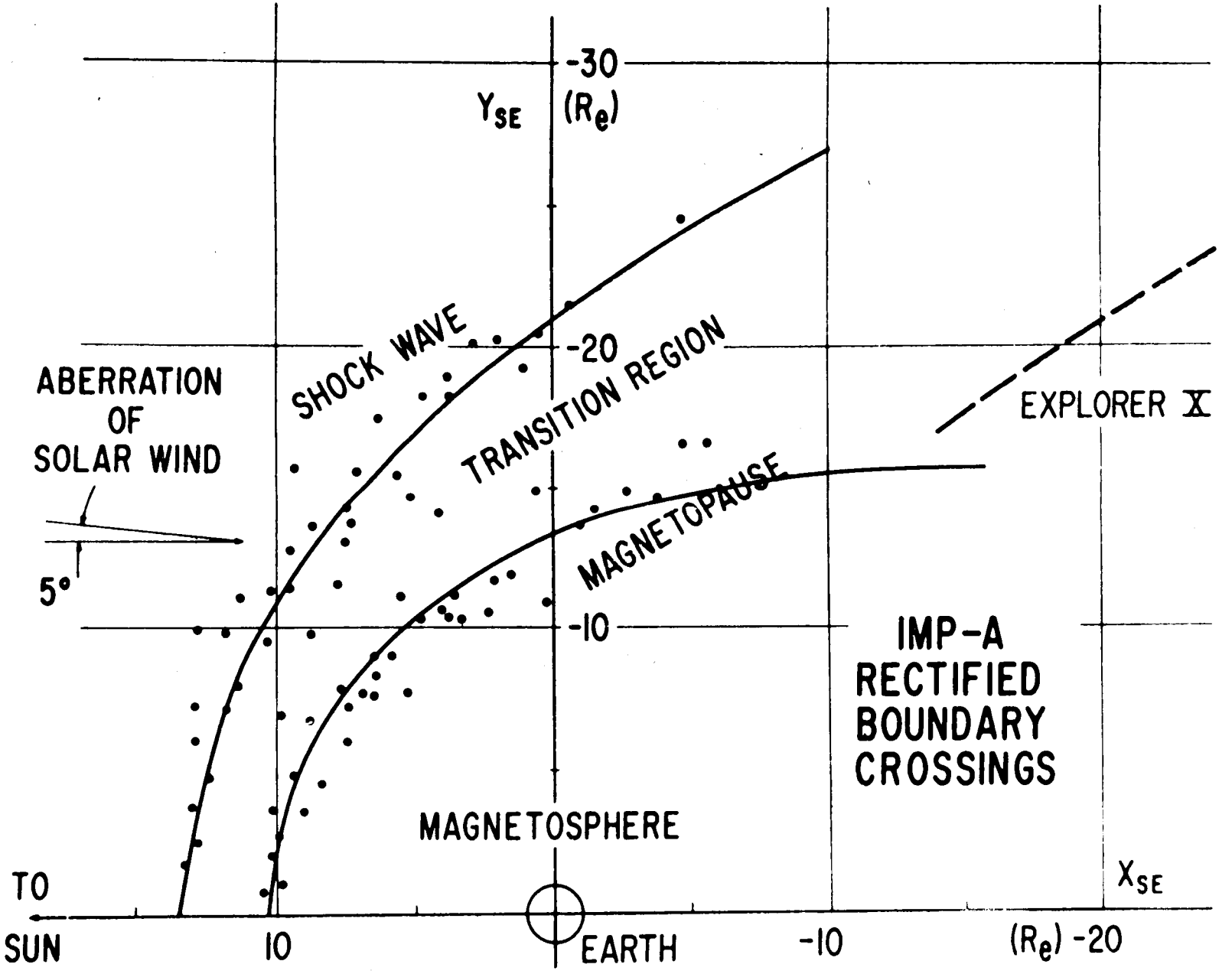
-30
Y_{SE} (R_e)
-20
-10
SHOCK WAVE
TRANSITION REGION
MAGNETOPAUSE
ABERRATION
OF
SOLAR WIND
5°
EXPLORER X
IMP-A
RECTIFIED
BOUNDARY
CROSSINGS
MAGNETOSPHERE
TO
SUN
10
EARTH
-10
(R_e) -20
X_{SE}

Figure 4

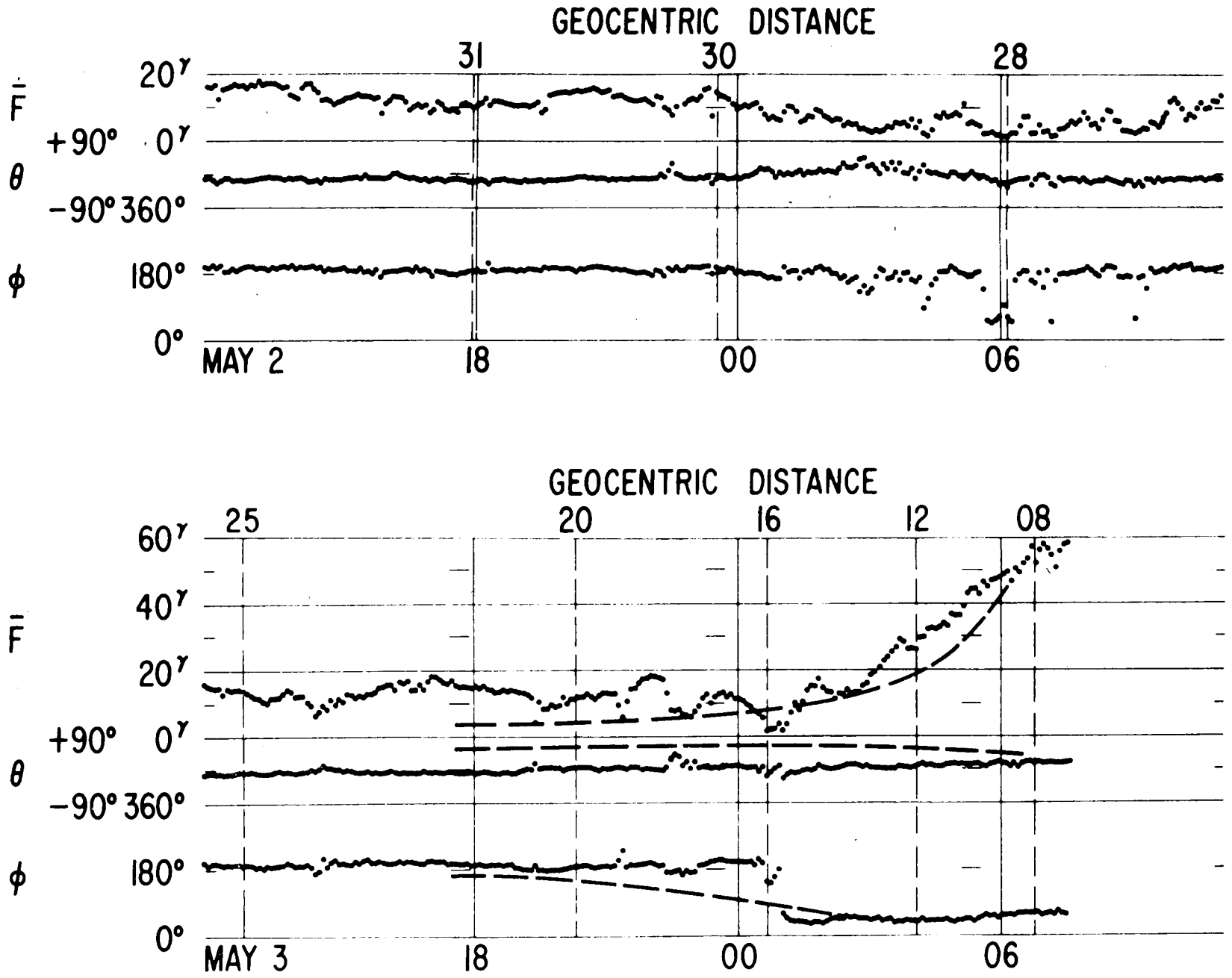

ORBIT NO. 41 IMP-I 1964

Figure 5

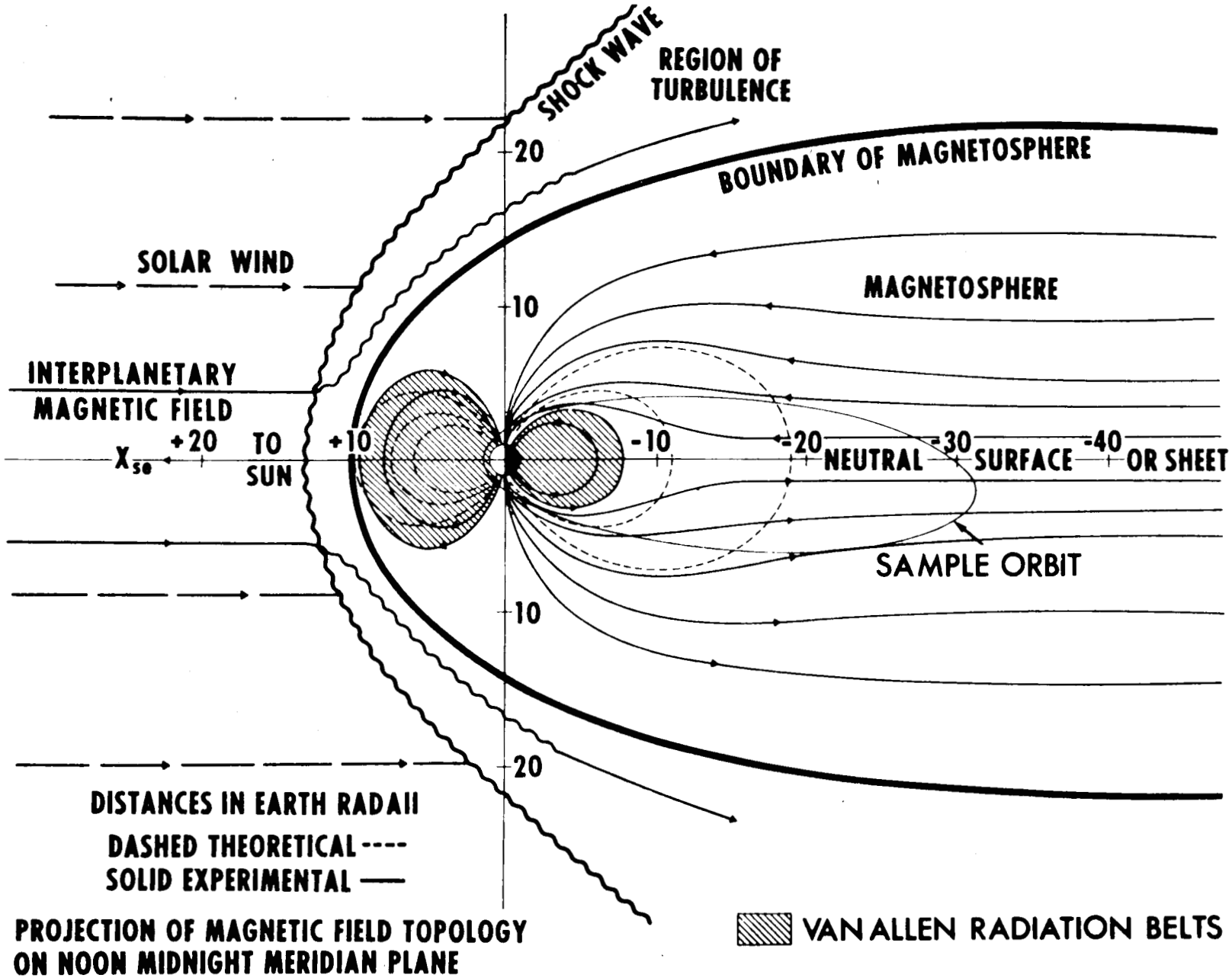
SHOCK WAVE
REGION OF TURBULENCE
BOUNDARY OF MAGNETOSPHERE
SOLAR WIND
MAGNETOSPHERE
INTERPLANETARY MAGNETIC FIELD
X_{se}
+20
+10
TO SUN
-10
-20
-30
-40
NEUTRAL SURFACE OR SHEET
SAMPLE ORBIT
20
10
10
20
DISTANCES IN EARTH RADAII
DASHED THEORETICAL ----
SOLID EXPERIMENTAL ——
PROJECTION OF MAGNETIC FIELD TOPOLOGY
ON NOON MIDNIGHT MERIDIAN PLANE
VAN ALLEN RADIATION BELTS

Figure 6

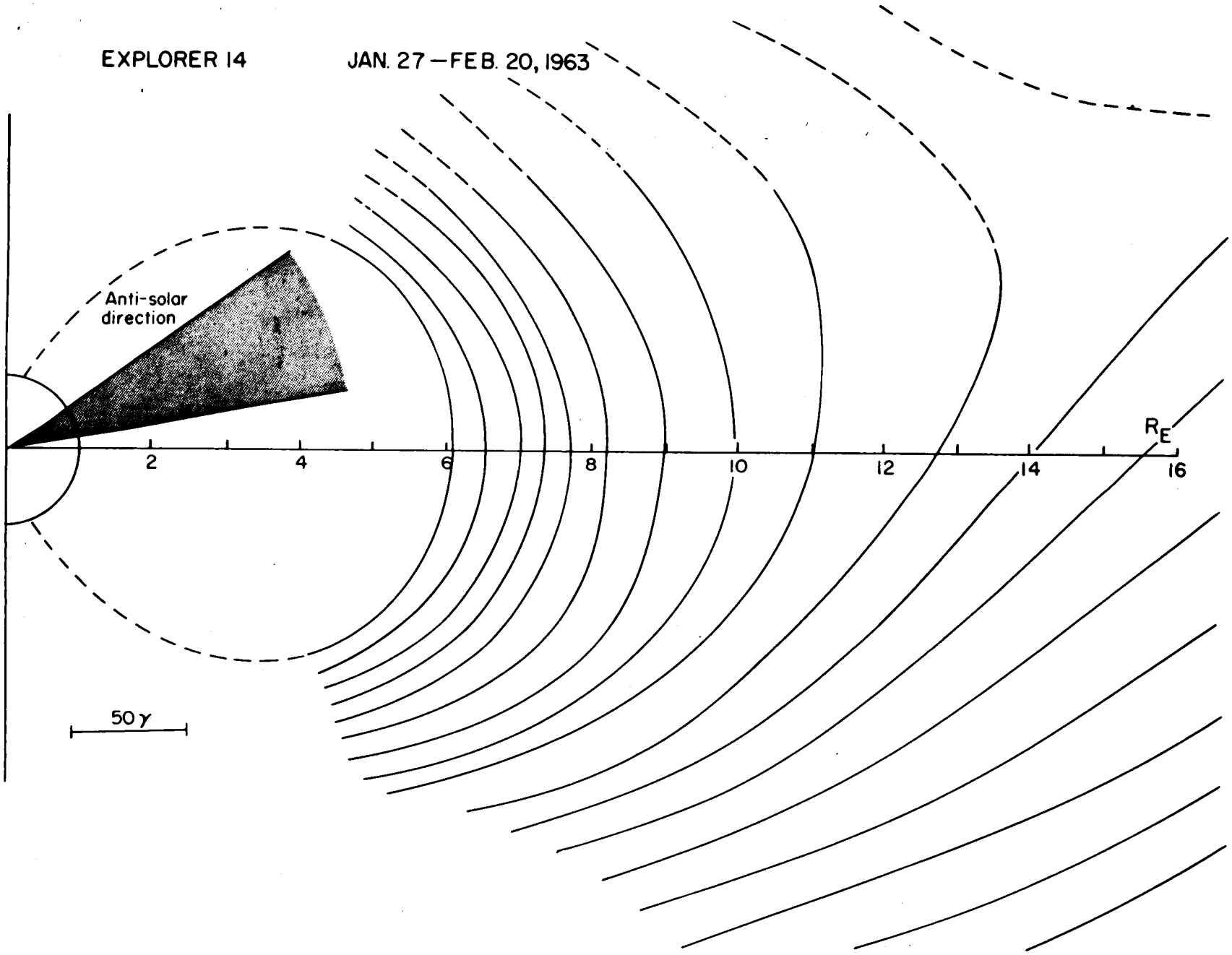
EXPLORER 14
JAN. 27 – FEB. 20, 1963
Anti-solar direction
2
4
6
8
10
12
14
16
R_E
50 γ

Figure 7

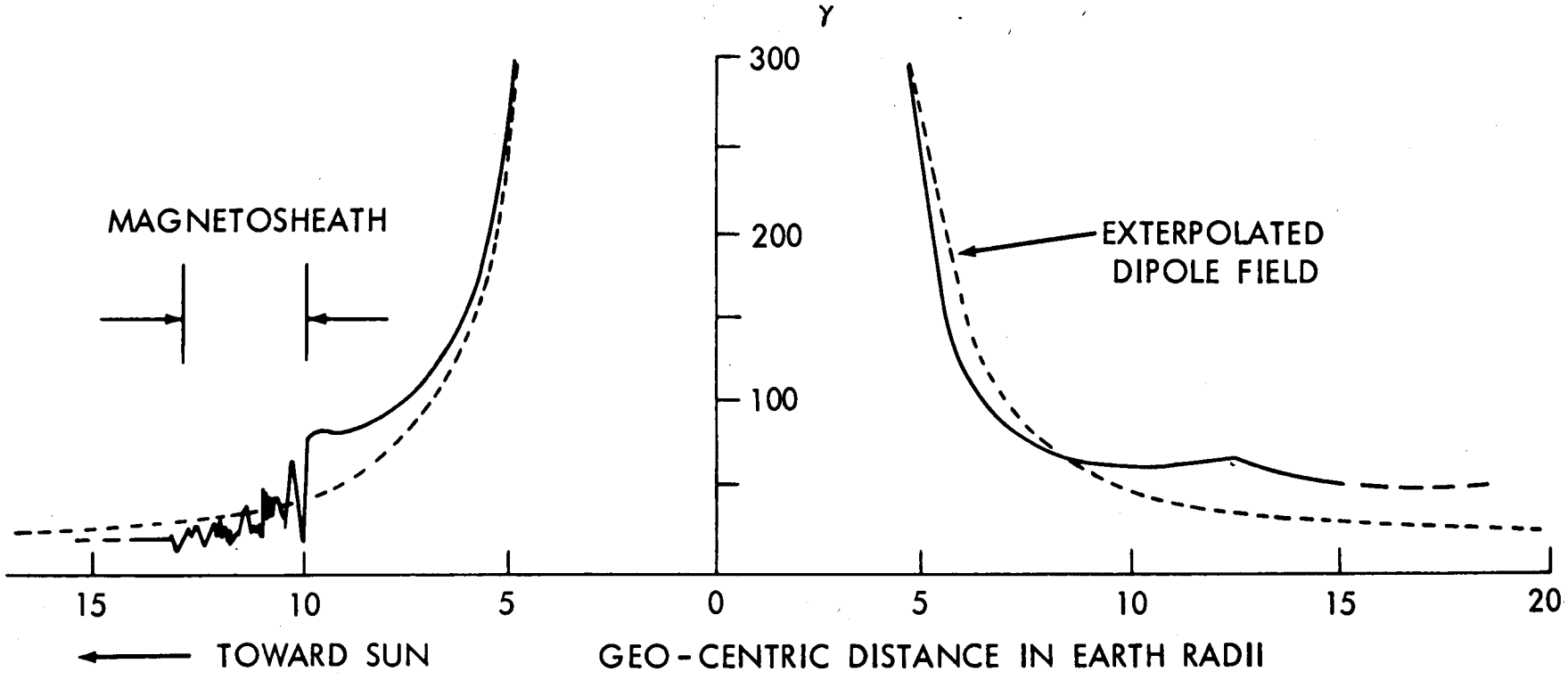

Schematic representation of the outer geomagnetic field in the equatorial plane along the sun-earth line.

Figure 8

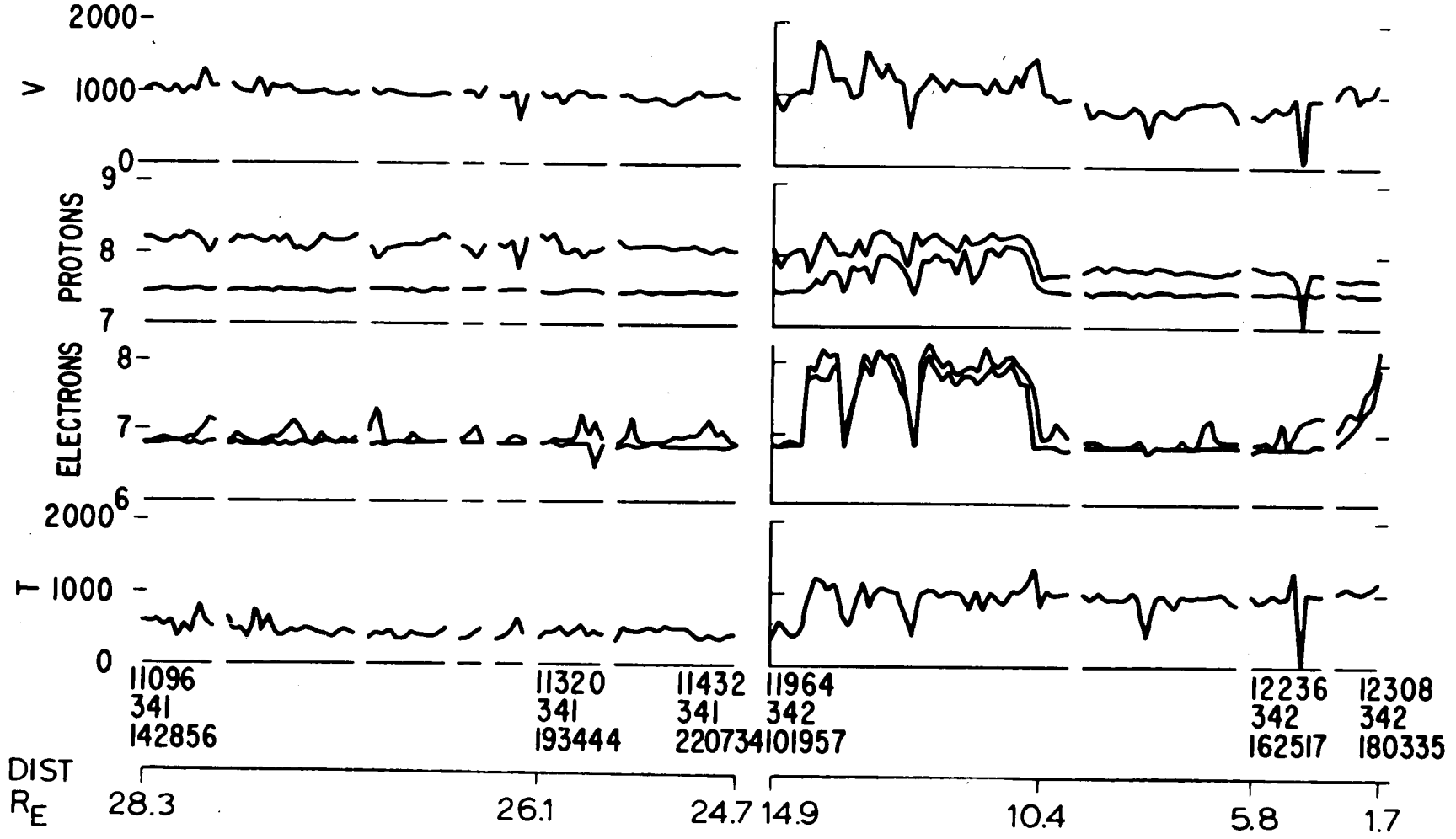
2000
> 1000
9^0
8
7
PROTONS
8
7
ELECTRONS
2000^6
1000
0
11096
341
142856
11320
341
193444
11432
341
220734
11964
342
101957
12236
342
162517
12308
342
180335
DIST
R_E
28.3
26.1
24.7
14.9
10.4
5.8
1.7

Figure 9

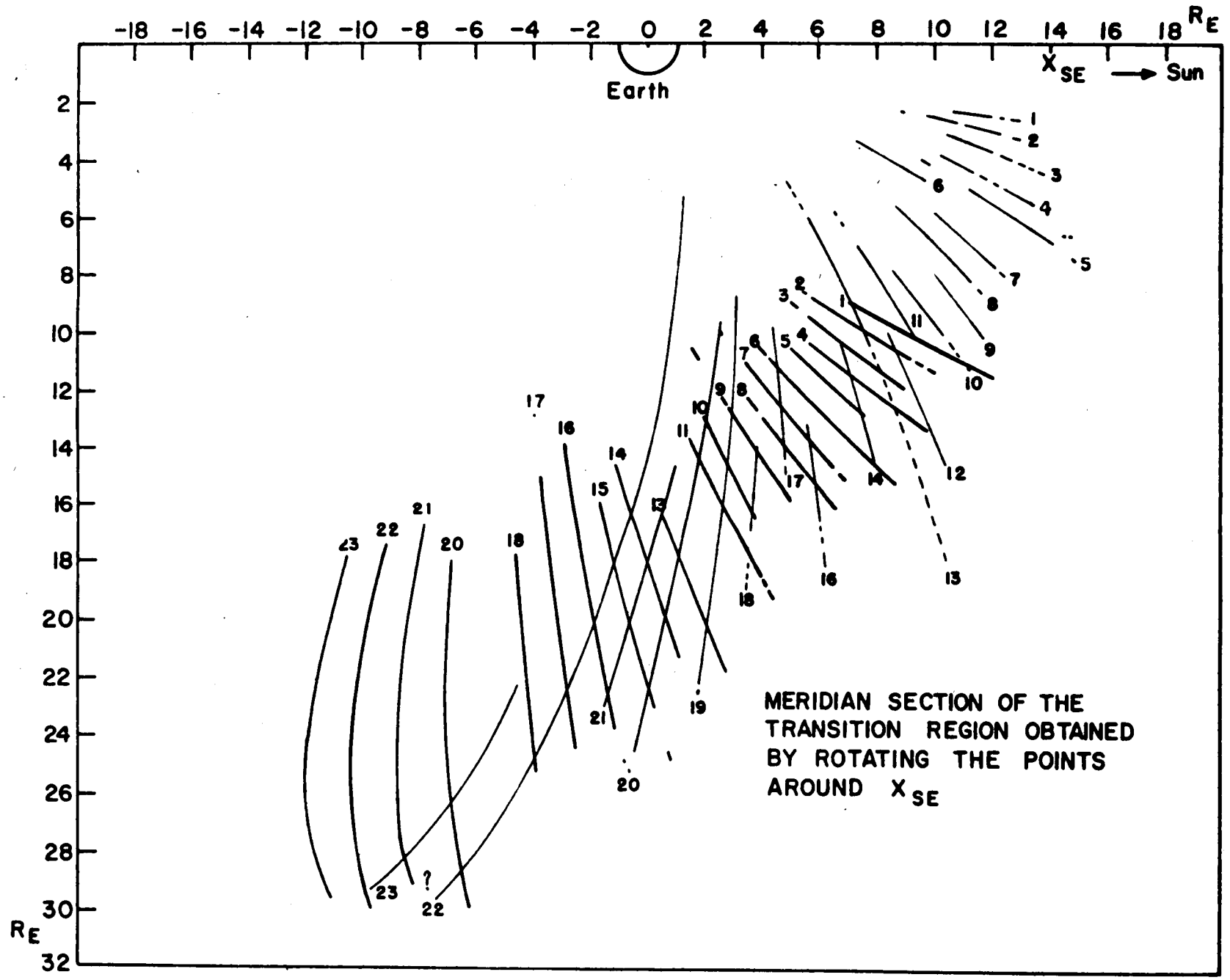
-18 -16 -14 -12 -10 -8 -6 -4 -2 0 2 4 6 8 10 12 14 16 18 R_E
X_{SE} → Sun
Earth
2 4 6 8 10 12 14 16 18 20 22 24 26 28 30 32
R_E
MERIDIAN SECTION OF THE TRANSITION REGION OBTAINED BY ROTATING THE POINTS AROUND X_{SE}

Figure 10

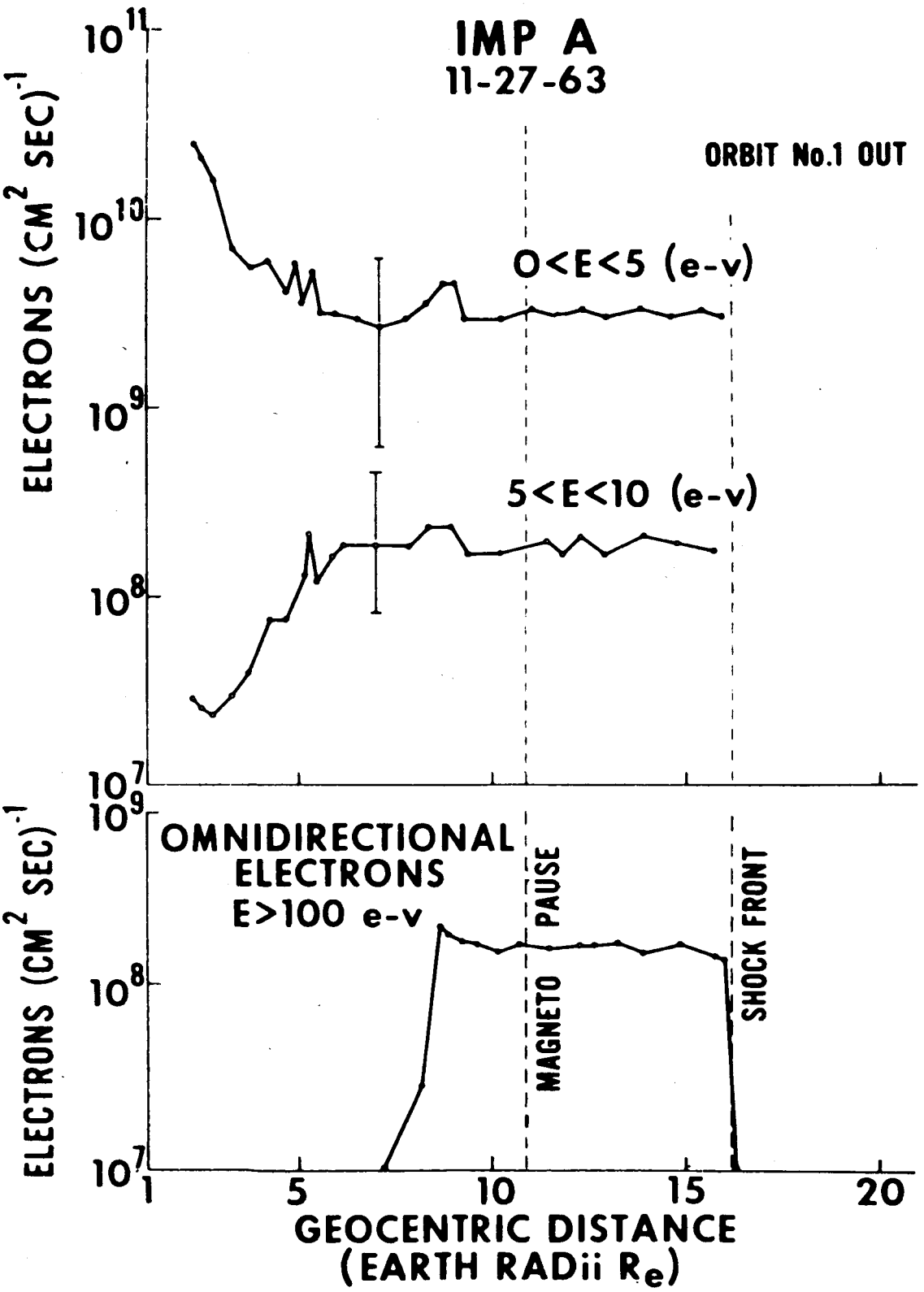
IMP A
11-27-63
ORBIT No.1 OUT
0<E<5 (e-v)
5<E<10 (e-v)
ELECTRONS (CM² SEC)⁻¹
OMNIDIRECTIONAL
ELECTRONS
E>100 e-v
MAGNETO PAUSE
SHOCK FRONT
GEOCENTRIC DISTANCE
(EARTH RADii Re)

Figure 11

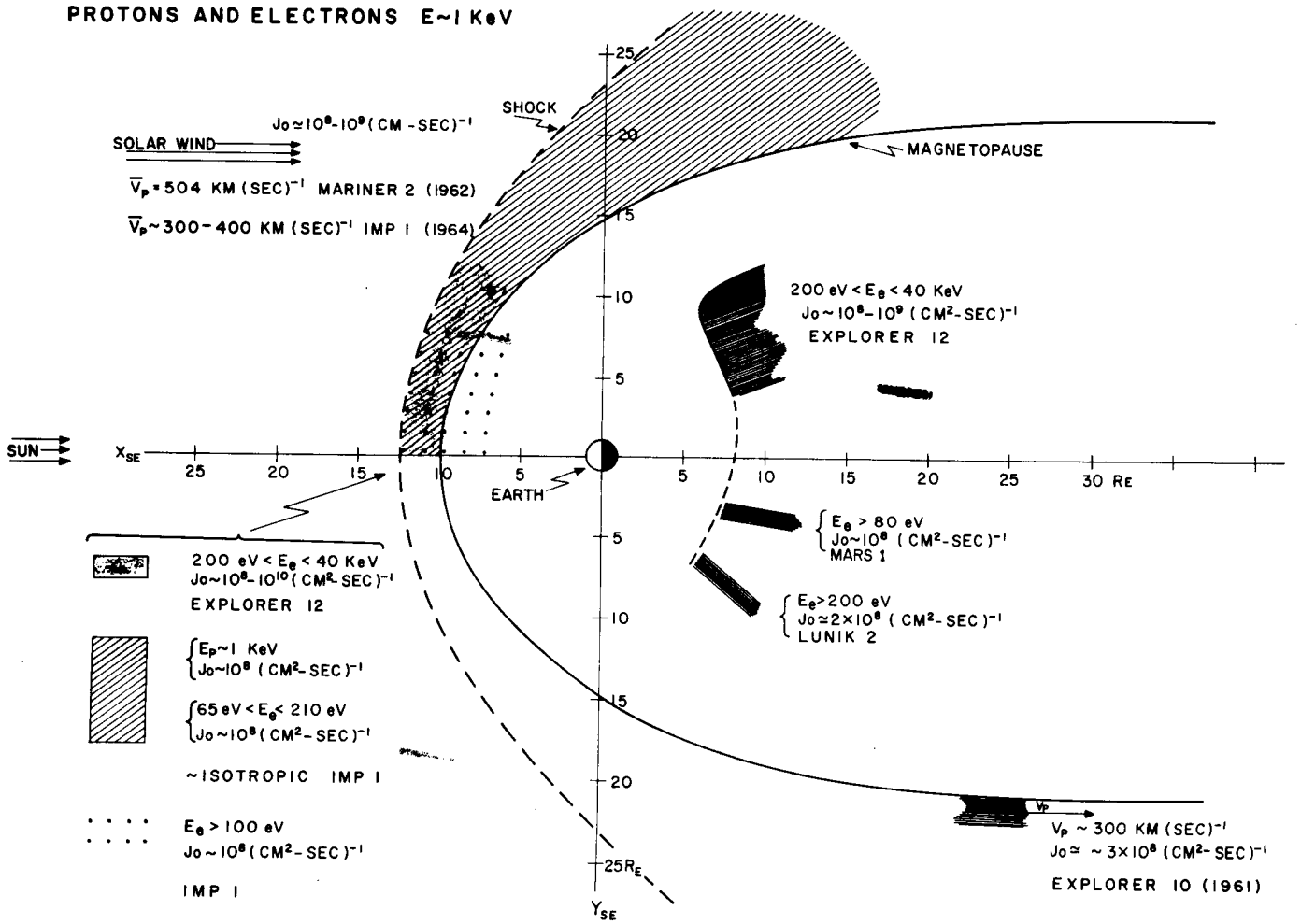
PROTONS AND ELECTRONS E~1 KeV
SHOCK
MAGNETOPAUSE
SOLAR WIND
Jo≃10⁸-10⁹ (CM-SEC)⁻¹
V̄p = 504 KM (SEC)⁻¹ MARINER 2 (1962)
V̄p ~ 300-400 KM (SEC)⁻¹ IMP 1 (1964)
200 eV < Ee < 40 KeV
Jo ~ 10⁸-10⁹ (CM²-SEC)⁻¹
EXPLORER 12
SUN
XSE
EARTH
30 RE
Ee > 80 eV
Jo~10⁸ (CM²-SEC)⁻¹
MARS 1
Ee>200 eV
Jo≃2×10⁸ (CM²-SEC)⁻¹
LUNIK 2
200 eV < Ee < 40 KeV
Jo~10⁸-10¹⁰ (CM²-SEC)⁻¹
EXPLORER 12
Ep~1 KeV
Jo~10⁸ (CM²-SEC)⁻¹
65 eV < Ee < 210 eV
Jo~10⁸ (CM²-SEC)⁻¹
~ISOTROPIC IMP 1
Ee > 100 eV
Jo ~ 10⁸ (CM²-SEC)⁻¹
IMP 1
Vp
Vp ~ 300 KM (SEC)⁻¹
Jo≃ ~3×10⁸ (CM²-SEC)⁻¹
EXPLORER 10 (1961)
25RE
YSE

Figure 12

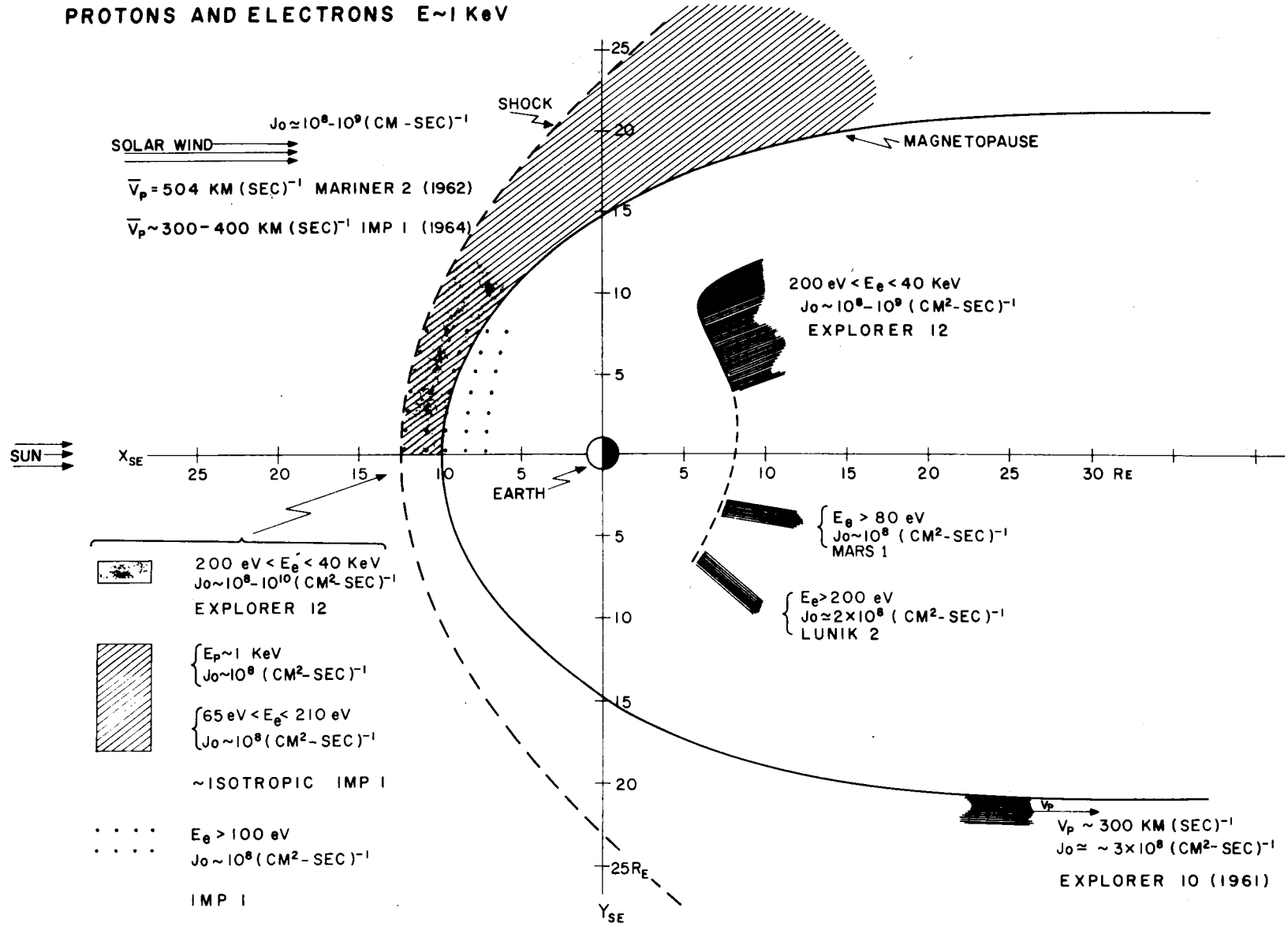
PROTONS AND ELECTRONS E~1 KeV
SHOCK
Jo≃10⁸-10⁹ (CM-SEC)⁻¹
SOLAR WIND
MAGNETOPAUSE
V̄p = 504 KM (SEC)⁻¹ MARINER 2 (1962)
V̄p ~ 300-400 KM (SEC)⁻¹ IMP 1 (1964)
200 eV < Ee < 40 KeV
Jo ~ 10⁸-10⁹ (CM²-SEC)⁻¹
EXPLORER 12
SUN
XSE
25 20 15 10 5 EARTH 5 10 15 20 25 30 RE
Ee > 80 eV
Jo~10⁸ (CM²-SEC)⁻¹
MARS 1
Ee>200 eV
Jo≃2×10⁸ (CM²-SEC)⁻¹
LUNIK 2
200 eV < Ee < 40 KeV
Jo~10⁸-10¹⁰ (CM²-SEC)⁻¹
EXPLORER 12
Ep~1 KeV
Jo~10⁸ (CM²-SEC)⁻¹
65 eV < Ee < 210 eV
Jo~10⁸ (CM²-SEC)⁻¹
~ISOTROPIC IMP 1
Ee > 100 eV
Jo~10⁸ (CM²-SEC)⁻¹
IMP 1
Vp
Vp ~ 300 KM (SEC)⁻¹
Jo≃ ~3×10⁸ (CM²-SEC)⁻¹
EXPLORER 10 (1961)
25RE
YSE

Figure 12

POSITIONS OF THE GEOMAGNETIC TRAPPING BOUNDARY AND OF THE TERMINATION OF ENERGETIC ELECTRONS IN THE TRANSITION REGION AS DETERMINED WITH EXPLORER XIV MEASUREMENTS OF ELECTRONS E > 40 KeV

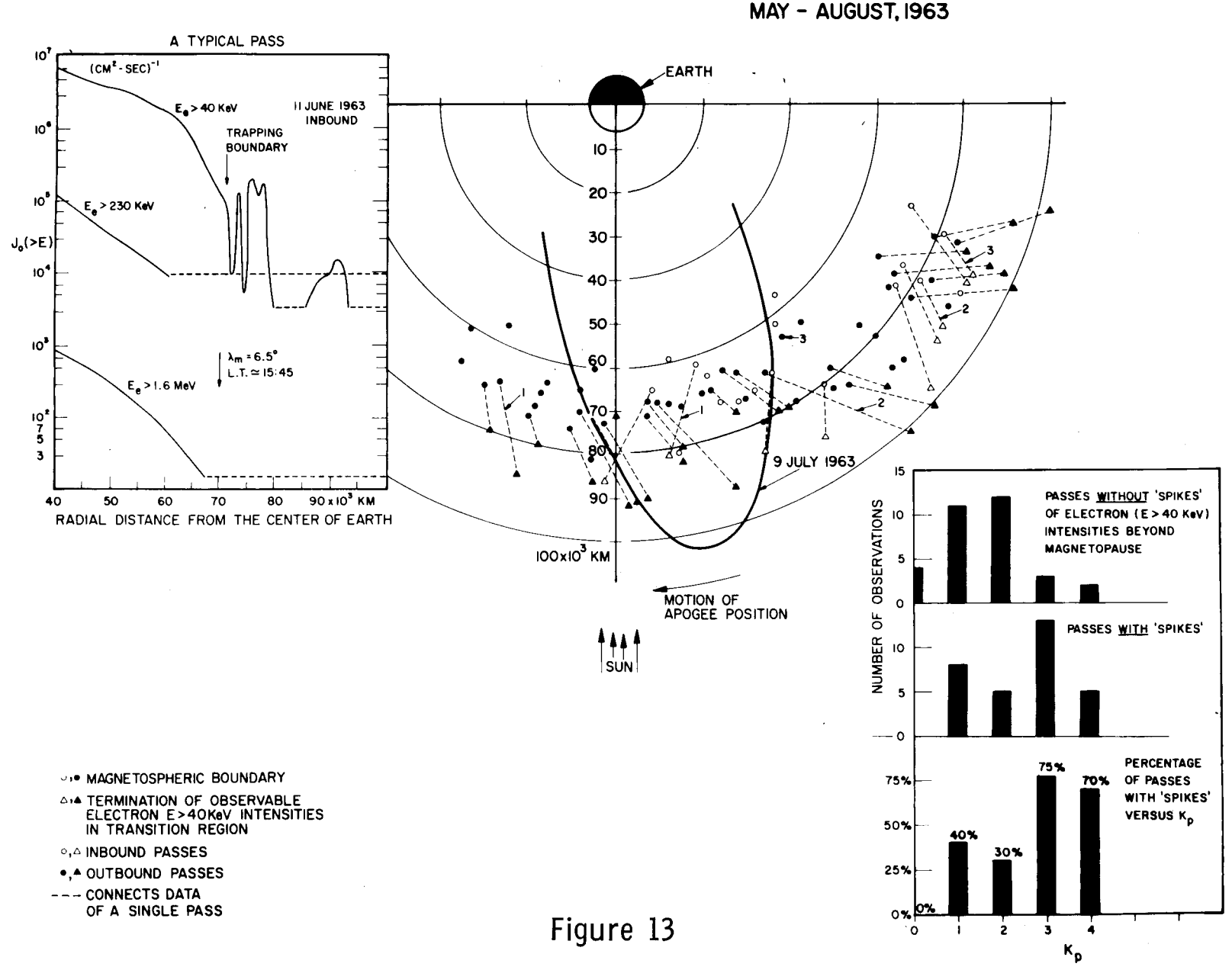

Figure 13

G 65-179

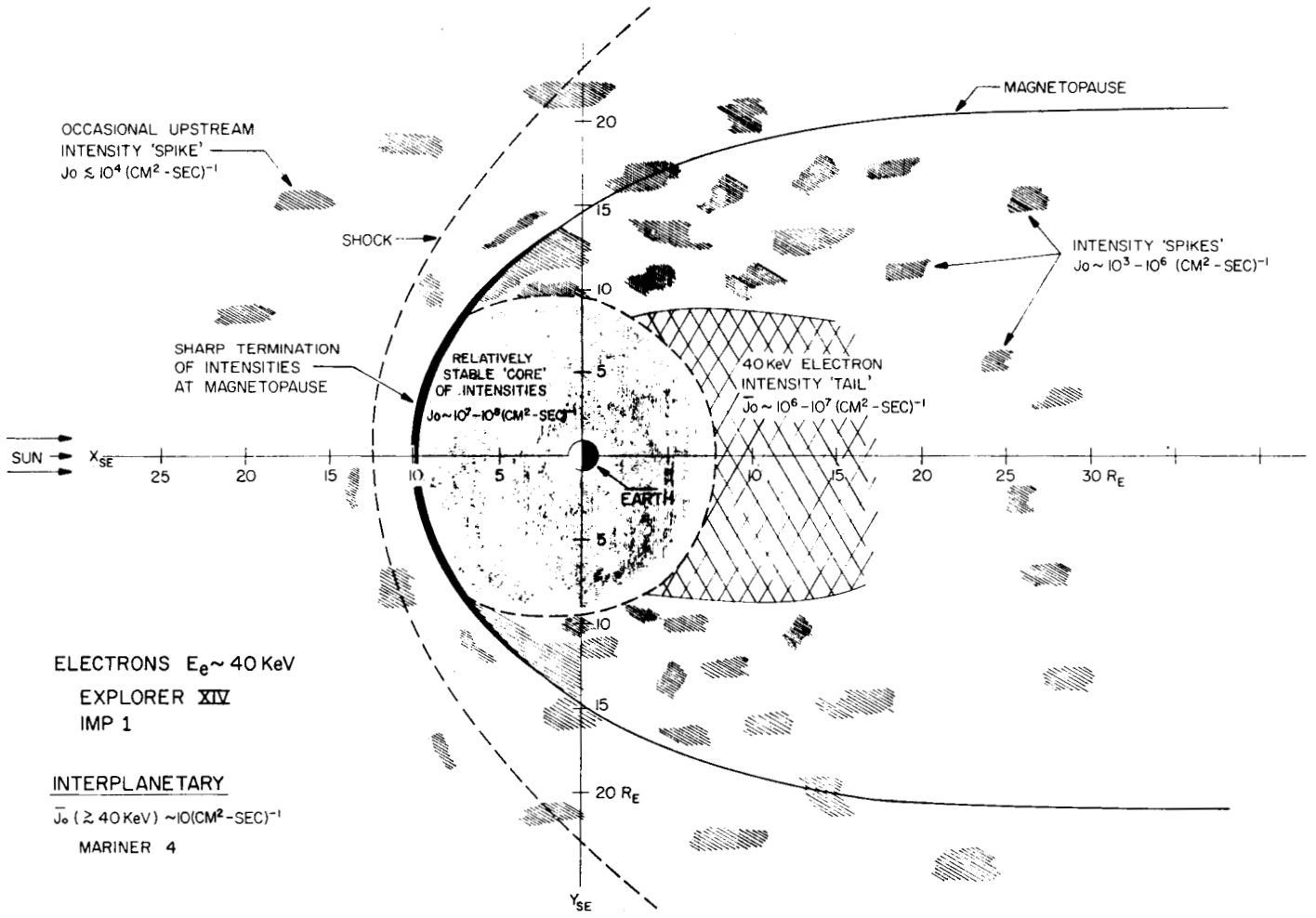

Figure 14

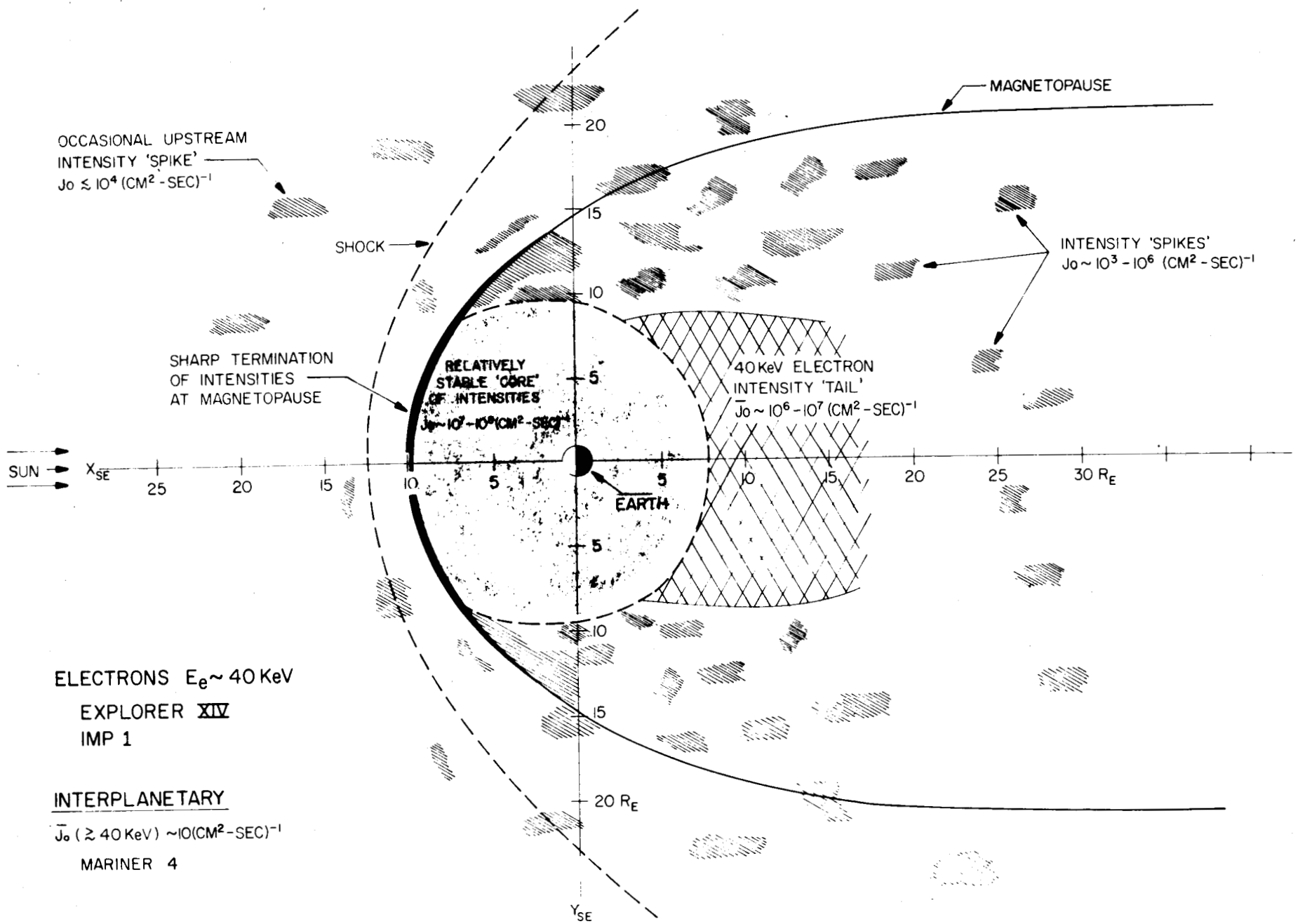
MAGNETOPAUSE
OCCASIONAL UPSTREAM
INTENSITY 'SPIKE'
Jo ≲ 10⁴ (CM² - SEC)⁻¹
SHOCK
INTENSITY 'SPIKES'
Jo ~ 10³ - 10⁶ (CM² - SEC)⁻¹
SHARP TERMINATION
OF INTENSITIES
AT MAGNETOPAUSE
RELATIVELY
STABLE 'CORE'
OF INTENSITIES
40 KeV ELECTRON
INTENSITY 'TAIL'
J̄o ~ 10⁶ - 10⁷ (CM² - SEC)⁻¹
SUN
X_SE
EARTH
Y_SE
30 R_E
20 R_E
ELECTRONS Eₑ ~ 40 KeV
EXPLORER XIV
IMP 1
INTERPLANETARY
J̄o (≳ 40 KeV) ~10(CM² - SEC)⁻¹
MARINER 4

Figure 14

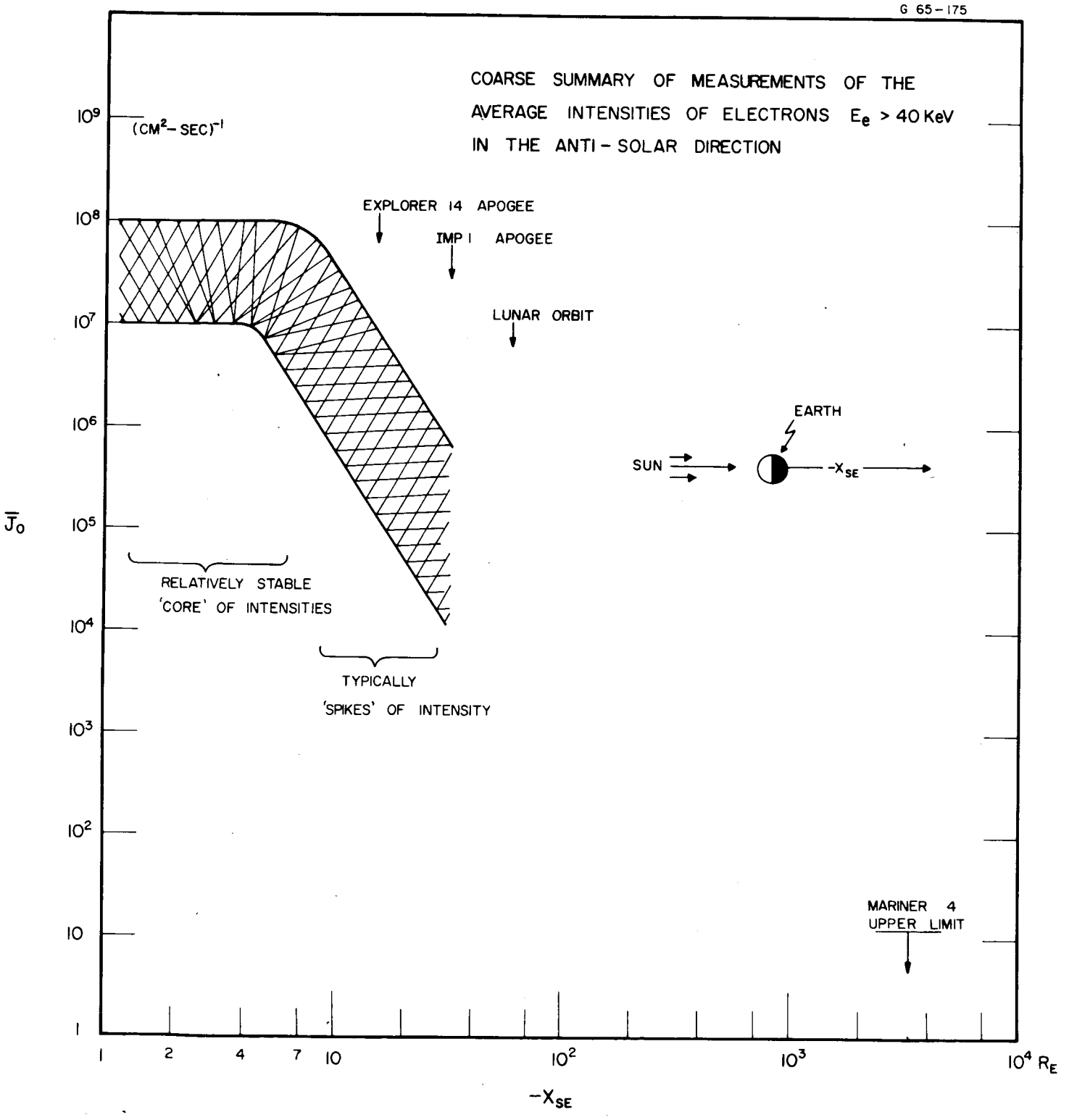
G 65-175
COARSE SUMMARY OF MEASUREMENTS OF THE AVERAGE INTENSITIES OF ELECTRONS E_e > 40 KeV IN THE ANTI-SOLAR DIRECTION
10^9
$(CM^2-SEC)^{-1}$
10^8
10^7
10^6
10^5
10^4
10^3
10^2
10
1
$\bar{J}_0$
EXPLORER 14 APOGEE
IMP I APOGEE
LUNAR ORBIT
EARTH
SUN
$-X_{SE}$
RELATIVELY STABLE 'CORE' OF INTENSITIES
TYPICALLY 'SPIKES' OF INTENSITY
MARINER 4 UPPER LIMIT
1
2
4
7
10
10^2
10^3
10^4 R_E
$-X_{SE}$

Figure 15

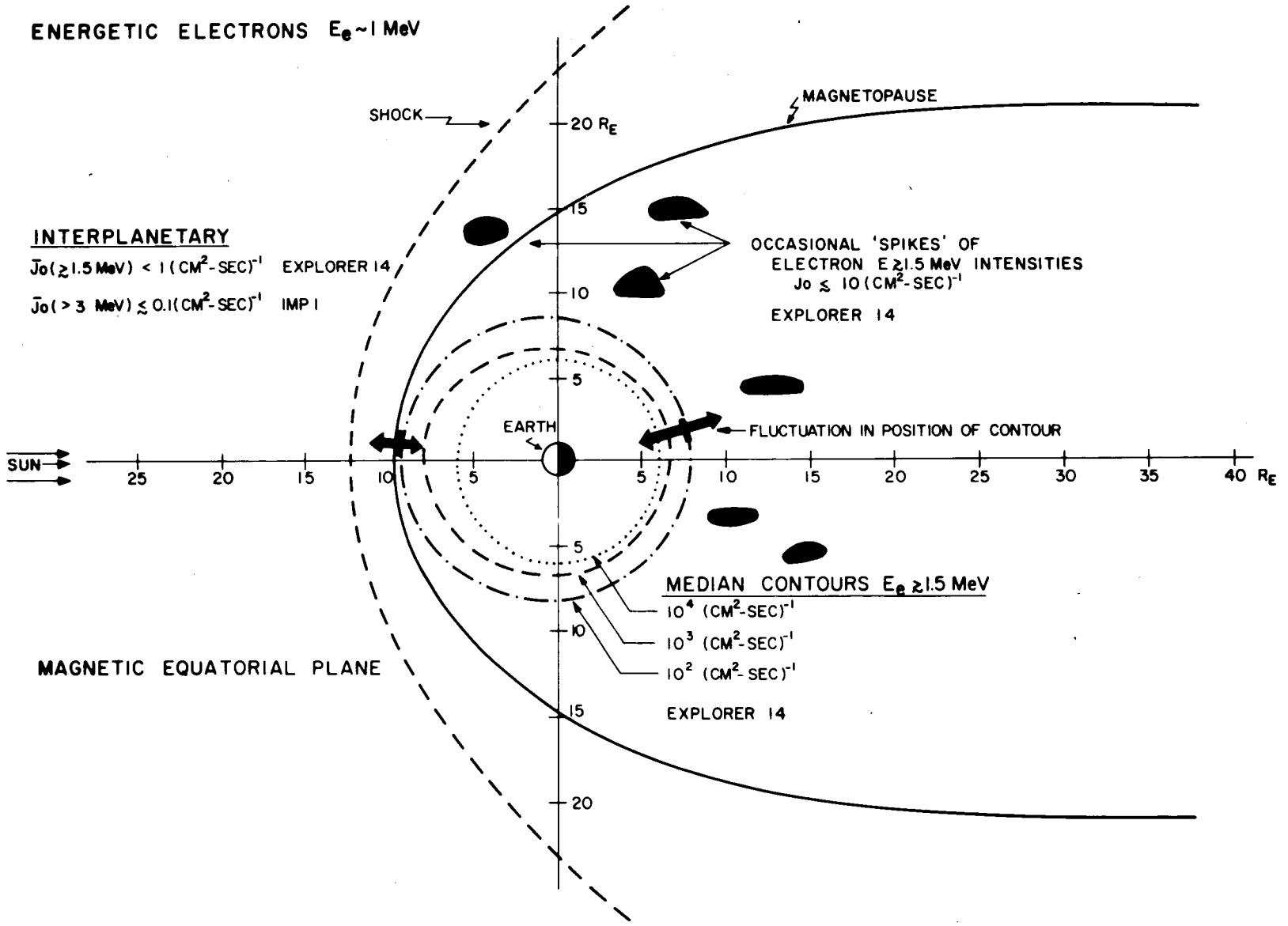
ENERGETIC ELECTRONS E_e~1 MeV
SHOCK
MAGNETOPAUSE
20 R_E
INTERPLANETARY
$\bar{J}o(\gtrsim 1.5\ MeV) < 1\ (CM^2\text{-}SEC)^{-1}$ EXPLORER 14
$\bar{J}o(>3\ MeV) \lesssim 0.1\ (CM^2\text{-}SEC)^{-1}$ IMP I
OCCASIONAL 'SPIKES' OF
ELECTRON E ≳1.5 MeV INTENSITIES
Jo ≲ 10 $(CM^2\text{-}SEC)^{-1}$
EXPLORER 14
EARTH
FLUCTUATION IN POSITION OF CONTOUR
SUN
25 20 15 10 5 5 10 15 20 25 30 35 40 R_E
MEDIAN CONTOURS $E_e \gtrsim 1.5$ MeV
$10^4\ (CM^2\text{-}SEC)^{-1}$
$10^3\ (CM^2\text{-}SEC)^{-1}$
$10^2\ (CM^2\text{-}SEC)^{-1}$
EXPLORER 14
MAGNETIC EQUATORIAL PLANE

Figure 16

UNCLASSIFIED

Security Classification

DOCUMENT CONTROL DATA - R&D

(Security classification of title, body of abstract and indexing annotation must be entered when the overall report is classified)

1. ORIGINATING ACTIVITY *(Corporate author)*

University of Iowa, Department of Physics and Astronomy

2a. REPORT SECURITY CLASSIFICATION

UNCLASSIFIED

2b. GROUP

3. REPORT TITLE

Observations of Magnetospheric Boundary Phenomena

4. DESCRIPTIVE NOTES *(Type of report and inclusive dates)*

Progress August 1965

5. AUTHOR(S) *(Last name, first name, initial)*

Frank, L. A.

6. REPORT DATE	7a. TOTAL NO. OF PAGES	7b. NO. OF REFS
August 1965	57	84

8a. CONTRACT OR GRANT NO.	9a. ORIGINATOR'S REPORT NUMBER(S)
Nonr-1509(06)	U. of Iowa 65-32
b. PROJECT NO.	
c.	9b. OTHER REPORT NO(S) *(Any other numbers that may be assigned this report)*
d.	

10. AVAILABILITY/LIMITATION NOTICES

Qualified requesters may obtain copies of this report from DDC.

11. SUPPLEMENTARY NOTES	12. SPONSORING MILITARY ACTIVITY
	Office of Naval Research

13. ABSTRACT

A brief summary of recent major observations of magnetospheric boundary phenomena is provided with emphasis on Explorers 12 and 14 and IMP 1 measurements of charged particles and of magnetic fields in the sunward magnetopause region and within the tail of the magnetosphere in the anti-solar direction. Major observations of charged particles in these regions are summarized in several equatorial spatial distribution diagrams.

DD FORM 1 JAN 64 1473

UNCLASSIFIED

Security Classification

14. KEY WORDS	LINK A		LINK B		LINK C	
	ROLE	WT	ROLE	WT	ROLE	WT
Observations of Magnetospheric Boundary Phenomena						

INSTRUCTIONS

1. ORIGINATING ACTIVITY: Enter the name and address of the contractor, subcontractor, grantee, Department of Defense activity or other organization *(corporate author)* issuing the report.

2a. REPORT SECURITY CLASSIFICATION: Enter the overall security classification of the report. Indicate whether "Restricted Data" is included. Marking is to be in accordance with appropriate security regulations.

2b. GROUP: Automatic downgrading is specified in DoD Directive 5200.10 and Armed Forces Industrial Manual. Enter the group number. Also, when applicable, show that optional markings have been used for Group 3 and Group 4 as authorized.

3. REPORT TITLE: Enter the complete report title in all capital letters. Titles in all cases should be unclassified. If a meaningful title cannot be selected without classification, show title classification in all capitals in parenthesis immediately following the title.

4. DESCRIPTIVE NOTES: If appropriate, enter the type of report, e.g., interim, progress, summary, annual, or final. Give the inclusive dates when a specific reporting period is covered.

5. AUTHOR(S): Enter the name(s) of author(s) as shown on or in the report. Enter last name, first name, middle initial. If military, show rank and branch of service. The name of the principal author is an absolute minimum requirement.

6. REPORT DATE: Enter the date of the report as day, month, year; or month, year. If more than one date appears on the report, use date of publication.

7a. TOTAL NUMBER OF PAGES: The total page count should follow normal pagination procedures, i.e., enter the number of pages containing information.

7b. NUMBER OF REFERENCES: Enter the total number of references cited in the report.

8a. CONTRACT OR GRANT NUMBER: If appropriate, enter the applicable number of the contract or grant under which the report was written.

8b, 8c, & 8d. PROJECT NUMBER: Enter the appropriate military department identification, such as project number, subproject number, system numbers, task number, etc.

9a. ORIGINATOR'S REPORT NUMBER(S): Enter the official report number by which the document will be identified and controlled by the originating activity. This number must be unique to this report.

9b. OTHER REPORT NUMBER(S): If the report has been assigned any other report numbers *(either by the originator or by the sponsor)*, also enter this number(s).

10. AVAILABILITY/LIMITATION NOTICES: Enter any limitations on further dissemination of the report, other than those imposed by security classification, using standard statements such as:

(1) "Qualified requesters may obtain copies of this report from DDC."

(2) "Foreign announcement and dissemination of this report by DDC is not authorized."

(3) "U. S. Government agencies may obtain copies of this report directly from DDC. Other qualified DDC users shall request through _____."

(4) "U. S. military agencies may obtain copies of this report directly from DDC. Other qualified users shall request through _____."

(5) "All distribution of this report is controlled. Qualified DDC users shall request through _____."

If the report has been furnished to the Office of Technical Services, Department of Commerce, for sale to the public, indicate this fact and enter the price, if known.

11. SUPPLEMENTARY NOTES: Use for additional explanatory notes.

12. SPONSORING MILITARY ACTIVITY: Enter the name of the departmental project office or laboratory sponsoring *(paying for)* the research and development. Include address.

13. ABSTRACT: Enter an abstract giving a brief and factual summary of the document indicative of the report, even though it may also appear elsewhere in the body of the technical report. If additional space is required, a continuation sheet shall be attached.

It is highly desirable that the abstract of classified reports be unclassified. Each paragraph of the abstract shall end with an indication of the military security classification of the information in the paragraph, represented as *(TS), (S), (C), or (U)*.

There is no limitation on the length of the abstract. However, the suggested length is from 150 to 225 words.

14. KEY WORDS: Key words are technically meaningful terms or short phrases that characterize a report and may be used as index entries for cataloging the report. Key words must be selected so that no security classification is required. Identifiers, such as equipment model designation, trade name, military project code name, geographic location, may be used as key words but will be followed by an indication of technical context. The assignment of links, roles, and weights is optional.